Volume 44, Number 1, 2018.

Mobility & Vehicle Mechanics

International Journal for Vehicle Mechanics, Engines and Transportation Systems

ISSN 1450 - 5304

UDC 621 + 629(05)=802.0

UNIVERSITY OF KRAGUJEVAC, FACULTY OF ENGINEERING

SERBIAN SOCIETY OF AUTOMOTIVE ENGINEERS

M V M **M**obility **V**ehicle **M**echanics

Editors: Prof. dr ***Jovanka Lukić****; Prof. dr* ***Čedomir Duboka***

MVM *Editorial Board*
University of Kragujevac
Faculty of Engineering
Sestre Janjić 6, 34000 Kragujevac, Serbia
Tel.: +381/34/335990; Fax: + 381/34/333192

For Publisher: Prof. dr Dobrica Milovanović, dean, University of Kragujevac, Faculty of Engineering

Publishing of this Journal is financially supported from:
Ministry of Education, Science and Technological Development, Republic Serbia

Mobility & **V**ehicle **M**echanics

Volume 44
Number 1
2018.

Motorna **V**ozila i **M**otori

Mobility & **V**ehicle **M**echanics

Volume 44
Number 1
2018.

Motorna **V**ozila i **M**otori

MOBILITY & VEHICLE MECHANICS

DOI: 10.24874/mvm.2018.44.01.01
UDC: 621.381:621.43

APPLICATION OF VARIOUS SIGNAL PROCESSING METHODS IN COMBUSTION ENGINES

Sunny Narayan [1], Ivan Grujic [2], Nadica Stojanovic [3], Kaisan Muhammad Usman [4], Abubakar Shitu [5], Faisal O. Mahroogi [6]*

Received: December 2017 Revised: January 2018 Accepted: March 2018

RESEARCH ARTICLE

ABSTRACT: Study of combustion process in engines often rely on various diagnosis techniques which are based on acquisition of in cylinder pressure. In this work various tests were conducted to analyse the working of a gasoline engine by varying the load, speed and amount of fuel injected inside the cylinder. Effects of varying these operational parameters on in cylinder pressure, heat release rate and rate of rise of in cylinder pressure was analysed.

KEY WORDS: Combustion Engines, Signal processing

PRIMENA RAZLIČITIH METODA OBRADE SIGNALA U MOTORIMA SA SAGOREVANJEM

REZIME: Proučavanje procesa sagorevanja u motorima često se oslanja na različite tehnike dijagnostike, koje se zasnivaju na akviziciji pritiska u cilindru. U ovom radu sprovedeni su različiti testovi za analizu rada benzinskih motora promenom opterećenja, brzine i količine ubrizganog goriva u cilindar. Analizirani su efekti promene ovih radnih parametara na pritisak u cilindru, brzinu oslobađanja toplote i brzinu porasta pritiska u cilindru.

KLJUČNE REČI: motori sa sagorevanjem, obrada signala

*[1] Sunny Narayan, Assist. prof., Qassim University, Buraydah, Saudi Arabia, arabia-rarekv@gmail.com, (*Corresponding author)*
[2] Ivan Grujic, M.Sc., assist., University of Kragujevac, Faculty of engineering, Sestre Janjić 6, 34000 Kragujevac, Serbia, ivan.grujic@kg.ac.rs
[3] Nadica Stojanović, M.Sc., assist., University of Kragujevac, Faculty of engineering, Sestre Janjić 6, 34000 Kragujevac, Serbia, nadica.stojanovic@kg.ac.rs
[4] Kaisan Muhammad Usman, PhD, Ahmadu Bello University, Department of Mechanical Engineering, Zaria, Nigeria, mukaisan@abu.edu.ng
[5] Abubakar Shitu, PhD, Ahmadu Bello University, Department of Mechanical Engineering, Zaria, Nigeria, abubakarshitu88@gmail.com
[6] Faisal O. Mahroogi, PhD, Qassim University, Faculty of engineering, Department of mechanical engineering, Saudi Arabia, prof2090@gmail.com

Intentionally blank

APPLICATION OF VARIOUS SIGNAL PROCESSING METHODS IN COMBUSTION ENGINES

Sunny Narayan, Ivan Grujic, Nadica Stojanovic, Kaisan Muhammad Usman, Abubakar Shitu, Faisal O. Mahroogi

1. INTRODUCTION

Signals representing the in cylinder pressure form an important feedback for diagnosis of combustion process in combustion engines [1]. Use of various piezo-electric transducers has paved way for easy acquisition of pressure data [2, 3]. These sensors work on principle that charge is generated in them due to mechanical deformation.

These sensors are based on Quartz or Ceramic materials like Lithium Niobate &Lead Titinate [4]. However these sensors are sensitive towards temperature variations. The charge generated in these sensors is directly proportional to applied force as well as first pressure derivative [5]. Some other advantages of these sensors include high cycle life (109 cycles), low pressure hysteresis, high pressure as well as temperature stability [6]. Positioning of pressure transducer also effects signals acquired [7]. The charge output from transducer is applied to amplifier which converts signals to proportional voltage.

There are cyclic variations in acquired signals which can be eliminated by cyclic averaging. Previous works have taken into consideration 46 [8], 10 [9], 64 [10] and 100 [11] cycles. These variations occur due to varying amount of fuel injected, combustion conditions and different types of fuel-air mixtures formed inside combustion chamber [12]. There are several errors in signal acquisition process owing to resonance process as well as transmission and conversion errors [13]. Hence suitable filters are needed to smoothen the signals before further calculations can be done.

2. BACKGROUND

Due to high efficiency, diesel engines have been a favourite choice for heavy duty applications including trucks. However they suffer from drawbacks of high noise, weight and vibrations. These engines are of two types:

- Direct Injection (D.I.) engines
- In direct Injection engines.

In the D.I. engines, the fuel is directly injected inside combustion chamber and due to lesser time for mixing, a heterogamous mixture consisting of both rich and lean parts is formed in the chamber. Modern diesel injection systems use multiple injection process to control emissions like soot and Nitrous oxide (NOx) formation. These generally use three phases of injection. namely pre-injection period, Main –injection period & post injection period as seen from figure 1.

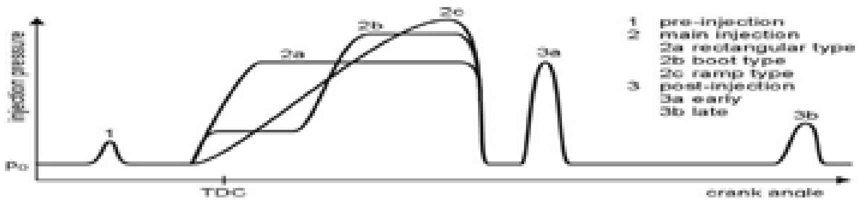

Figure 1. Multiple Injection process in diesel Engines

There is delay period between the start of ignition process and fuel injected inside diesel engine. More this ignition delay, more is the temperature during combustion and hence better condition for NOx formation. To shorten the delay period, small amount of fuel is pre-injection before main injection during the phase pre-Mixed combustion phase. The torque and power produced in engine depends upon main injection period. It is advantageous to vary injected fuel mass with time to reduce the specific fuel consumption. This method is known as rate shaping as depicted in figure 1. Rate shaping may be rectangular, step or boot in shape. Post-injection of fuel is done to reduce soot emissions and in some cases may be useful for exhaust gas recirculation treatment of gases [16]. It has been reported that post injection reduces soot by about 70% without increasing the fuel consumption [16].

3. EXPERIMENTAL SETUP

Experiments were conducted on single cylinder diesel engine. The engine test rig have Dytran Model Series 2300V LIVM pressure transducer for in cylinder pressure measurements and an optical crank angle encoder for detection of TDC position as well as engine speed. The given system can do maximum of 2 injections per cycle.

A Behringer ECM8000 type microphone was used to record the block noise. During the tests variations in injection timings and duration of injection was carried out. The data recorded during each test was under steady state conditions as seen in Table 1. All signals were acquired for a complete cycle of operation of engine.

Table 1. Injection parameters

CASE	Q_{pre} (mm^3/stroke)	Q_{main} (mm^3/stroke)	SOI_{pre} (Degree before TDC)	SOI_{main} (Degree before TDC)
B1	1	6.3	19.9°	5.09°
B2	1	13.9	14.6°	6.29°
B3	-	-	-	-
B4	1	6.6	22.5°	5.68°
B5	1	13.8	16.5°	6.29°
B6	-	-	-	-

Measurement installation is shown on Figure 2.

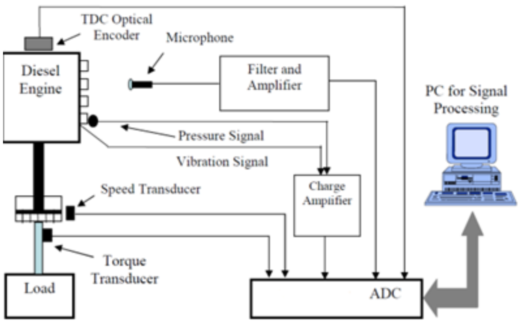

Figure 2. Measurement installation

4. RESULTS AND DISCUSION

Figures 3 and 4, show the variations of raw voltage signals obtained from amplifier for a single cycle of diesel engine with crank angles for various testing conditions.

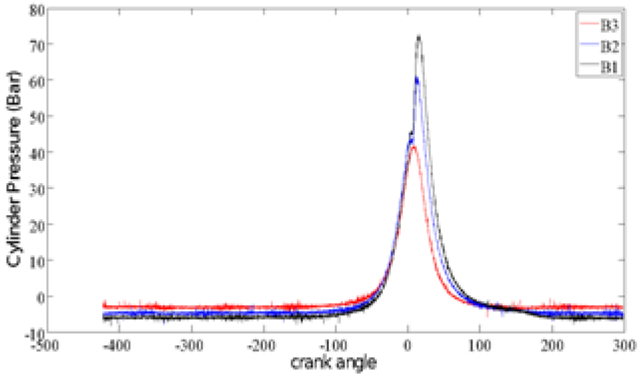

Figure 3. In cylinder pressure trace for various testing

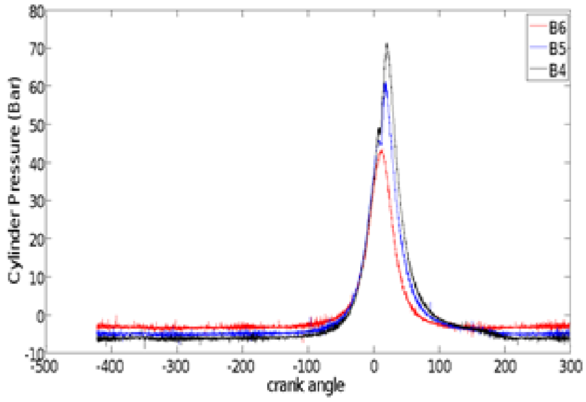

Figure 4. In cylinder pressure trace for various testing

It can be observed that depending upon engine speed/load condition, the intensity of maximum pressure and its location on crank angle domain changes. The data was converted from crank angle domain into time domain using relevant sampling rate & then pressure spectrum was plotted using FFT analysis. Figure 5 shows such plot. The signals acquired were filtered to avoid aliasing. The peak value of spectrum was observed to at a frequency of 316 KHz. The cylinder pressure spectrum was found to be load and speed dependent. In cylinder pressure provides most valuable information about combustion process occurring in engines. Piezo electric sensors have fast response time, small size and low sensitivity to surroundings, hence they are more suited to measure cylinder pressure in combustion chambers [17]. Several factors like noise due to pressure signal transmission and conversion, analog to digital conversion and variation in engine input parameters effect the pressure measurements. Oscillations are also caused by pressure waves in the cylinder which are picked up by the sensors.

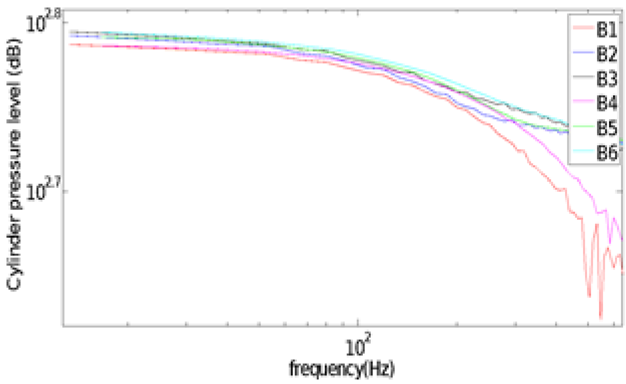

Figure 5. In cylinder pressure levels

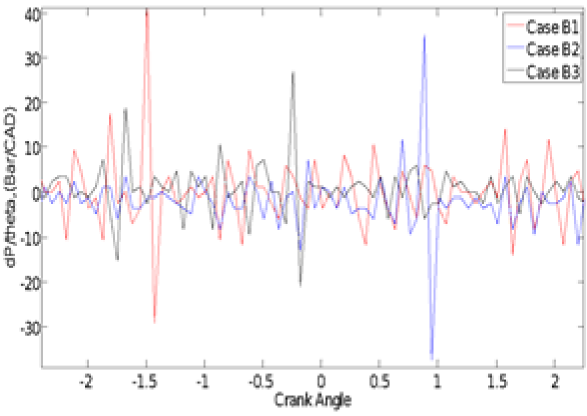

Figure 6. Rate of cylinder pressure rise

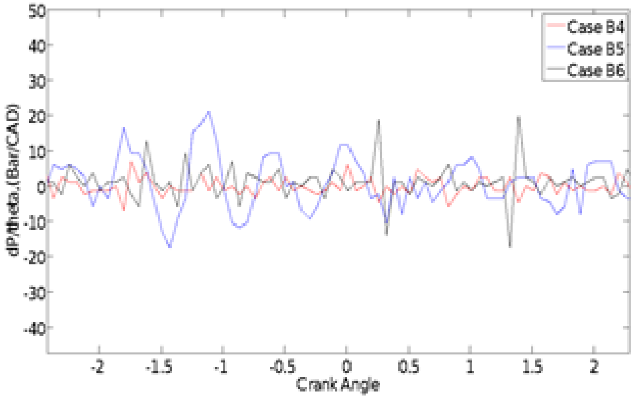

Figure 7. Rate of cylinder pressure rise

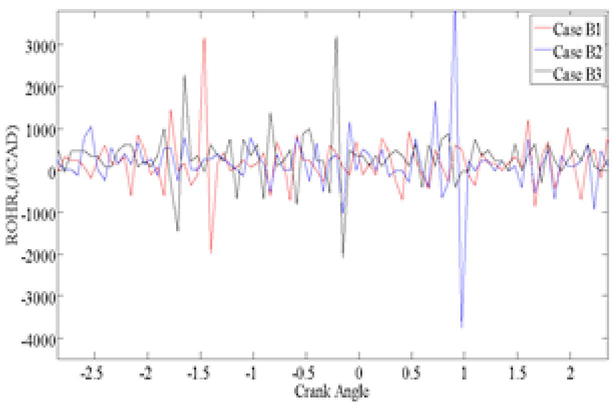

Figure 8. Rate of Heat Release Rate

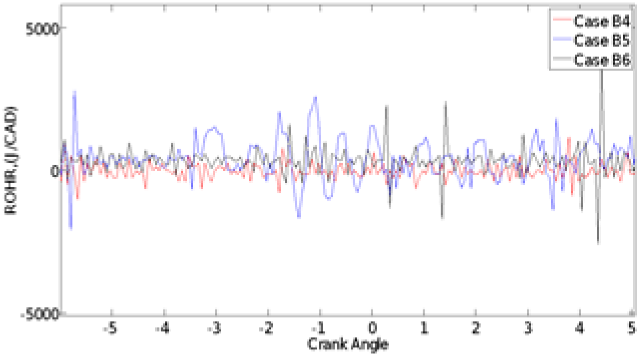

Figure 9. Rate of Heat Release Rate

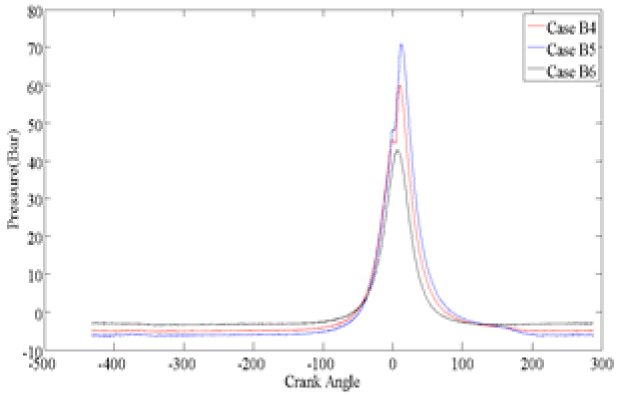

Figure 10. Filtered in cylinder pressure trace for various testing conditions

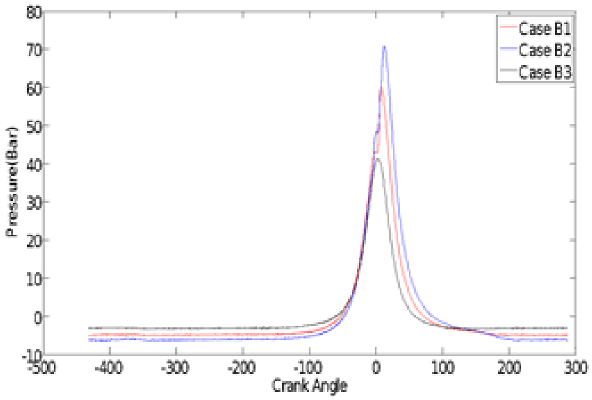

Figure 11. Filtered in cylinder pressure trace for various testing conditions

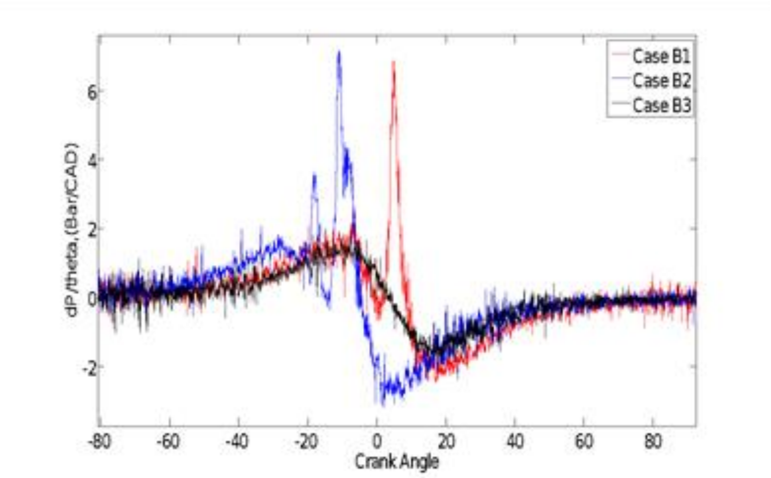

Figure 12. Filtered rate of cylinder pressure rise

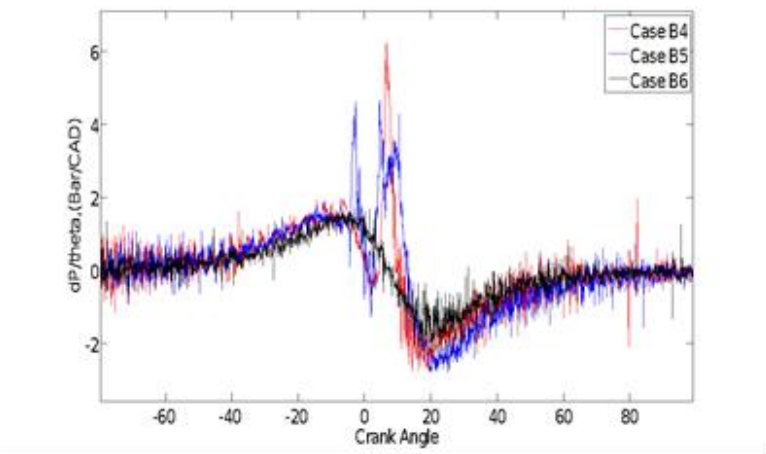

Figure 13. Filtered Rate of Cylinder Pressure Rise

The effects of noise are visible in pressure derivative curves. The oscillations in heat release rate curves are much more than pressure derivative curves. For correct visualization of combustion process it is necessary to filter the pressure data acquired. This was done by applying Savitzky-Golay filters. Figures 14 and 15 show the smoothened signals obtained by applying such a filter of third order. Since all the high frequency components are removed the remaining signals (having amplitude lesser than unfiltered signals) provide a useful information about combustion diagnosis. It can be seen from the curves that ROHR is almost zero outside combustion zone for case of filtered signals whereas for unfiltered one such values are high. It is needed that ROHR must be zero outside combustion zone as no fuel is burnt in this duration and hence no heat release rate is observed in combustion chamber.

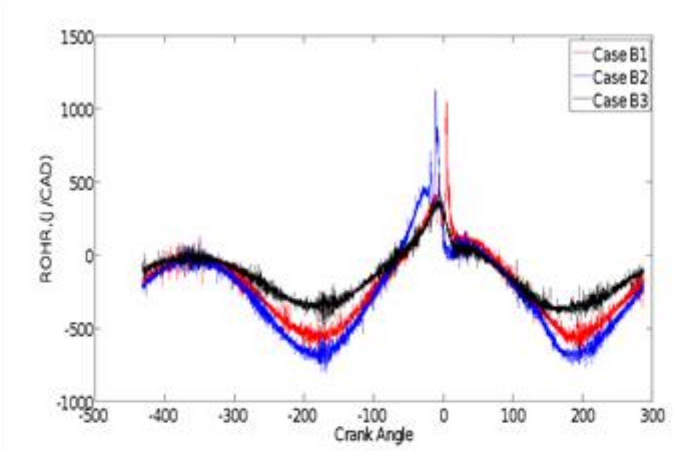

Figure 14. Filtered Rate of heat release rate

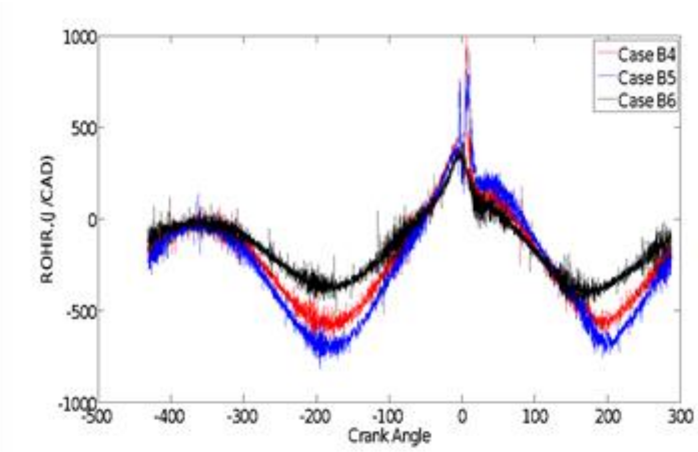

Figure 15. Filtered Rate of heat release rate

Several filters are available to filter digital signals which include butter worthy filter, zero phase & Savitzky-Golay etc. Figure 16 shows the effects of various filters applied on power spectrum of in cylinder pressure for case of test case B1. It is evident from this figure that Golay filters remove high frequency components more compared with other filters. In order to reduce the effects of cyclic variations optimum number of cycles are to be determined which depend upon engine type & operating conditions [18]. Using standard deviation of cylinder pressure signals. Figure 17 shows the standard deviation evolution for 20 cycles for the test condition B1.

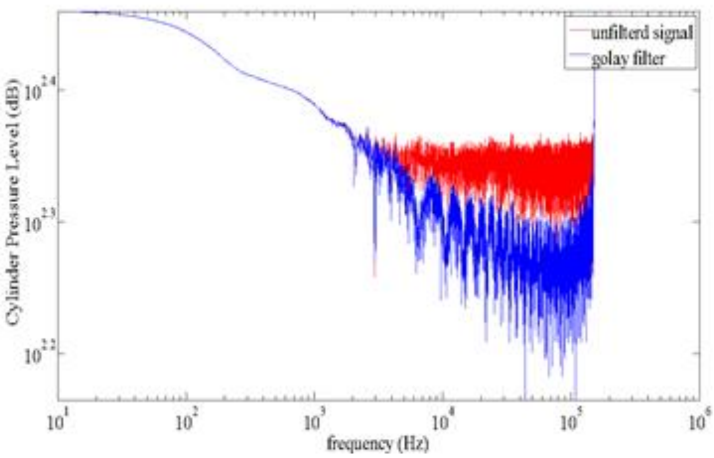

Figure 16. Effect of filtering on signals

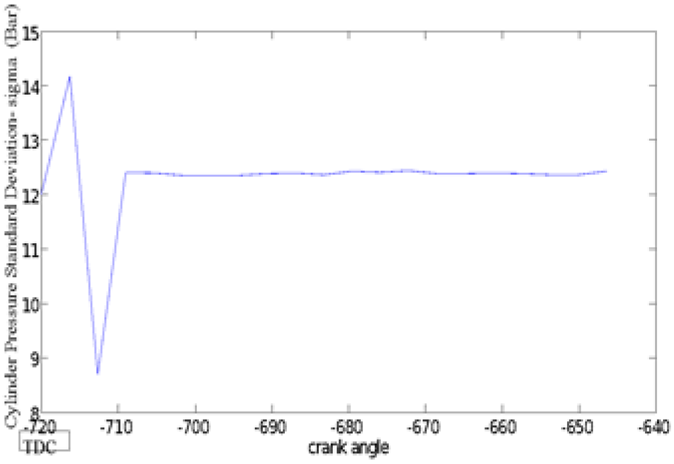

Figure 17. Standard deviation for pressure data

As it is evident from this graph, the standard deviation of pressure strongly depends upon the crank angle with large variations found near TDC position. This is because of combustion process occurring itself has large variations owing to no control over auto ignition of charge, combustion conditions and variations. In physical as well as chemical properties of charge formed in the combustion chamber. Hence filtered pressure data depicts the actual standard deviation as seen from figure 18.

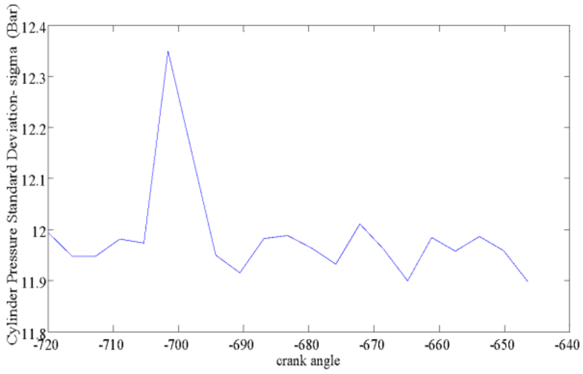

Figure 18. Standard deviation for filtered pressure data

The difference between maximum and minimum values of standard deviation data was found to decrease with an increase in number of cycles used. A point has been reported in [13] wherein increase in the number of cycles used does not change this difference. Hence after this point increasing the number of cycles does not improve the precision of results. Hence it can be concluded that optimum number of cycles are dependent upon engine operating conditions & smoothing methods used. ROHR provides an insight of how chemical energy of fuel is converted into thermal energy, hence an important tool in combustion diagnosis. So correct calculation of this curve is essential. Figure no 18 shows standard deviation of ROHR curves for the test condition B1 using data from 5 engine cycles. Reduction in these values was found when filtered signal data was applied in calculations as seen from figure no 19.

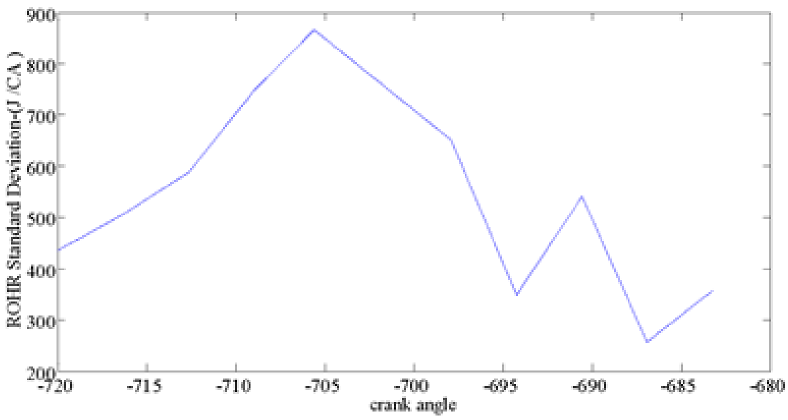

Figure 19. Standard deviation for ROHR data

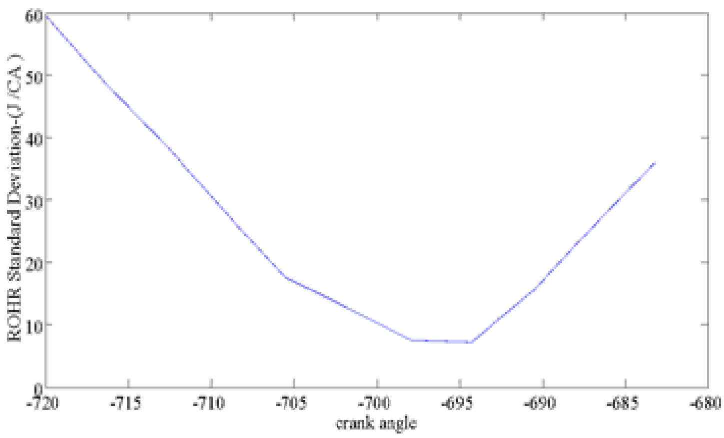

Figure 20. Filtered standard deviation for ROHR data

5. CONCLUSIONS

Experiments were done on a diesel engine operating at different engine conditions. The cylinder pressure data was measured for 20 consecutive engine cycles for analysis using piezoelectric pressure sensor. The cylinder pressure signals shows cyclic variations therefore signals were to smoothen to remove high frequency noise arising from various sources. This smoothened data was then used for calculating of ROHR and analyzing engine combustion. Variations in pressure signals increase with mixture enrichment. Oscillations in pressure traces during compression stroke are fairly small as compared to those originating from the combustion process. Averaging several cycles of pressure signals reduces the point-to-point variation due to signal noise. Optimum number of cycles to be used for combustion analysis is decided based on cycle-to-cycle standard deviation of pressure, rate of pressure rise and rate of heat release curves.

In the tested operating conditions of engine used for the study, optimal number is found to be 5 cycles while using Savitzky–Golay filter for smoothening the pressure signals. Savitzky–Golay filter is superior in performance compared to zero phase filter and Butterworth filter, while analyzing the signals.

REFERENCES

[1] Murya, R., Datt, D., D., Aggarwal, A., Digital signal processing of cylinder pressure data for combustion diagnosis of HCCI engine, Mechanical Systems and Signal Processing, 2013; 36(1), 95-109, doi: 10.1016/j.ymssp.2011.07.014.

[2] Leonhardt, S., Muller, N., Isermann, R., Methods for engine supervision and control using cylinder pressure information, ASME Transactions on Mechatronics, 1999, 4(3), 235-245, doi: 10.1109/3516.789682.

[3] Yoon, M., Lee, K., Sunwoo, M., A method for combustion phasing control using cylinder pressure measurement in a CRDI Diesel Engine, Mechatronics, 2007, 17(9), 469-479, doi: 10.1016/j.mechatronics.2007.06.001.

[4] Shimasaki, Y., Kobayashi, M., Sakamoto, H., Ueno, M., Study on engine management system using in cylinder pressure sensor integrated with spark plug, SAE Technical Paper, 2004, 2004-01-0519, 22, doi: https://doi.org/10.4271/2004-01-0519.

[5] Eastwood, P., Combustion sensors, Momentum press, New Jersey, 1999.

[6] Tudor, M., Beeby, P., Automotive sensors, Momentum press, New Jersey, 2009.

[7] Hountalas, T., Anetis, A., Effect of pressure transducer position on measured cylinder pressure diagram of high speed diesel engines, Energy Conversion and Management, 1998, 39(7), 589-607, doi: https://doi.org/10.1016/S0196-8904(97)10009-7.

[8] RE Velation, Operator Reference Manual, Hi-Techniques Inc, Madison, 2004, 81-96.

[9] Chen, Z., Konno, M., Oguma, M., Yanai, T., Experimental study of CI natural gas /DME air mixtures in a homogenous charge engine, SAE Paper, 2000, 2000-01-0329, doi: https://doi.org/10.4271/2000-01-0329.

[10] Lida, N., Igarashi, T., Auto ignition and combustion of N butane and DME/air mixtures in a homogeneous Charge Compression Ignition Engine, SAE Paper, 2000, 2000-01-1832, doi: https://doi.org/10.4271/2000-01-1832.

[11] Murya, R., Datt, Dev Dutt, Aggarwal, A., Experimental study of combustion and Emission characteristic of ethanol fuelled port injected homogeneous charge compression ignition engine, Applied Energy, 2011, 88(4), 1169-1180, doi: 10.1016/j.apenergy.2010.09.015.

[12] Payri, F., Lujan, M., Martin, J., Abbad, A., Digital Signal processing of in cylinder pressure for combustion diagnosis of internal combustion engines, Mechanical System and Signal Processing, 2010, 24(8), 1767-1784, doi: 10.1016/j.ymssp.2009.12.011.

[13] Payri, F., Broatch, A., Tormos, B., Marant, V., New methodology for in cylinder pressure analysis in direct injection diesel engines-application to combustion noise, Measurement Science and Technology, 2005, 16(2), 540-547, doi: 10.1088/0957-0233/16/2/029.

[14] Stojanović, N., Glišović J., Lukić J., Grujić I., Influence of vanes shape on the high frequency noise of ventilated disc brakes in heavy vehicles, Mobility & Vehicle Mechanics, 2017, 43(4), doi: 10.24874/mvm.2017.43.03.01, 2017.

[15] Grujić, I., Lukić J., Miloradović D., Davinić A., Stojanović N., Identification of combustion noise, 13th International Conference on Accomplishments in Mechanical and Industrial Engineering-DEMI, Banja Luka, Repubika Srpska, 2017, 729-732, doi:

[16] Baumgarten, C., Mixture Formation in Internal Combustion Engines, Springer-Verlag Berlin Heidelberg, New York, 2006.

[17] Kangyoon, L., Maru, Y., Myoungho, S., A study on pegging methods for noisy cylinder pressure signal, Control Engineering Practice, 2008, 16(8), 922-929, doi:

[18] Murya, R., Datt, D.,D., Aggarwal, A., Experimental investigation on the effect of intake air temperature and air-fuel ratio on cycle to cycle variations in combustion and performance parameters, Applied Energy, 2011, 88(4), 1153-1163.

MOBILITY & VEHICLE MECHANICS

DOI: 10.24874/mvm.2018.44.01.02
UDC: 539.379(086.48)

DESIGN AND ANALYSIS OF AN AUTOMOTIVE SINGLE PLATE CLUTCH

Sunny Narayan [1*], *Ivan Grujic* [2], *Nadica Stojanovic* [3], *Kaisan Muhammad Usman* [4], *Abubakar Shitu* [5], *Faisal O. Mahroogi* [6]

Received in February 2018 Revised 23 February 2018 Accepted 2 April 2018

RESEARCH ARTICLE

ABSTRACT: This paper presents the stresses and deformations of the assembly of the automotive single plate clutch depending on the applied materials. Structural analysis of the clutch was performed by using the finite element method for a repressive vehicle example - Toyota KUN 25. First, the input data for the numerical analysis was calculated. Numerical analysis was performed in the ANSYS software package. As a result, the values of stresses and deformations that occur on the clutch during the vehicle exploitation are obtained.

KEY WORDS: stress, deformation, material, ANSYS, vehicle exploitation

DIZAJN I ANALIZA AUTOMOBILSKE JEDNODISKOSNE SPOJNICE

REZIME: Ovaj rad predstavlja prikaz napona i deformacije sklopa automobilske jednodiskosne spojnice u zavisnosti od primenjenog materijala. Strukturna analiza spojnice izvršena je metodom konačnih elemenata za reperezetni primer vozila – Toyota KUN 25. Najpre su proračunati polazni podaci za numeričku analizu. Numerička analiza izvršena je u softverskom paketu ANSYS. Kao rezultat dobijene su vrednosti napona i deformacija koje se javljaju na spojnici u toku eksploatacije vozila.

KLJUČNE REČI: motori sa sagorevanjem, obrada signala

[1] *Sunny Narayan, Assist. prof., Qassim University, Buraydah, Saudi Arabia, arabia-rarekv@gmail.com, (*Corresponding author)*
[2] *Ivan Grujic, M.Sc., assist., University of Kragujevac, Faculty of engineering, Sestre Janjić 6, 34000 Kragujevac, Serbia, ivan.grujic@kg.ac.rs*
[3] *Nadica Stojanović, M.Sc., assist., University of Kragujevac, Faculty of engineering, Sestre Janjić 6, 34000 Kragujevac, Serbia, nadica.stojanovic@kg.ac.rs*
[4] *Kaisan Muhammad Usman, PhD, Ahmadu Bello University, Department of Mechanical Engineering, Zaria, Nigeria, mukaisan@abu.edu.ng*
[5] *Abubakar Shitu, PhD, Ahmadu Bello University, Department of Mechanical Engineering, Zaria, Nigeria, abubakarshitu88@gmail.com*
[6] *Faisal O. Mahroogi, PhD, Qassim University, Faculty of engineering, Department of mechanical engineering, Saudi Arabia, prof2090@gmail.com*

Intentionally blank

DESIGN AND ANALYSIS OF AN AUTOMOTIVE SINGLE PLATE CLUTCH

Sunny Narayan, Ivan Grujic, Nadica Stojanovic, Kaisan Muhammad Usman, Abubakar Shitu, Faisal O. Mahroogi

1. INTRODUCTION

A clutch is a machine member used on the transmission shafts. Some friction plates, sometimes known as clutch plates are kept between these two members. This whole assembly is known as clutch as seen in Figure 1.
The clutch is based on the friction. When two friction surfaces brought in contact and pressed, then they are united due to friction force between them. This is the basic principle of clutch Narayan S. [1]. The friction between these two surfaces depends on the area of surface, pressure applied upon them and the friction material between them.

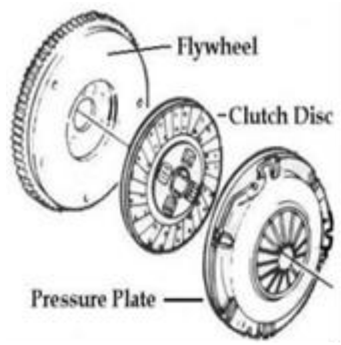

Figure 1. Clutch and flywheel [2]

The driving member of a clutch is the flywheel mounted on the engine crankshaft and the driven member is pressure plate mounted driving shaft to the driven shaft so that the driven shaft may be started or stopped at will, without stopping the driving as shown by Narayan S. [3, 4]. There are three states in which clutch can be found. These states are disengaged, clutch slipping and engaged. In automobile, a gearbox is required to change the speed and torque of the vehicle as analysed by Buzzoni [5] and Fang [6]. If we change a gear, when the engine is engaged with gearbox or when the gears are in running position then it can cause of wear and tear of gears. To overcome this problem a clutch is used between gearbox and engine. Clutch is the first element of power train. The main function of clutch is to engage and disengage the engine to transmission, when the driver need or during shifting of gear. When the clutch is in engaged position, the power flows from the engine to the wheel and when it is in disengage position, the power is not transmitted as seen by Zhao et al. [7].

The two main types of clutch are: positive clutch and friction clutch. Positive clutches are used when positive drive is required. The simplest type of a positive clutch is a jaw or claw clutch. A friction clutch has its principal application in the transmission of power of shafts and machines which must be started and stopped frequently. The force of friction is used to start the driven shaft from rest and gradually brings it up to the proper speed without excessive slipping of the friction surfaces. In automobiles, friction clutch is used to connect the engine to the drive shaft. The primary aim of this work is to design a rigid drive clutch system that meets multiple objectives such as Structural strength.

Gradual engagement clutches like the friction clutches are widely used in automotive applications for the transmission of torque from the flywheel to the transmission. The three major components of a clutch system are the clutch disc, the flywheel and the pressure plate. Flywheel is directly connected to the engine's crankshaft and hence rotates at the engine rpm. Bolted to the clutch flywheel is the second major component: the clutch pressure plate. The spring-loaded pressure plate has two jobs: to hold the clutch assembly together and to release tension that allows the assembly to rotate freely. Between the flywheel and the pressure plate is the clutch disc. The clutch disc has friction surfaces similar to a brake pad on both sides that make or break contact with the metal flywheel and pressure plate surfaces, allowing for smooth engagement and disengagement.

Gradual engagement clutches like the friction clutches are widely used in automotive application for the transmission of torque from the flywheel to the transmission. The three major components of a clutch system are the clutch disc, the flywheel and the pressure plate. Flywheel is directly connected to the engine's crankshaft and hence rotates at the engine RPM. Bolted to the clutch flywheel is the second major component:

the clutch pressure plate. The spring-loaded pressure plate has two jobs: to hold the clutch assembly together and to release tension that allows the assembly to rotate freely. Between the flywheel and the pressure plate is the clutch disc. The clutch disc has friction surfaces similar to a brake pad on both sides that make or break contact with the metal flywheel and pressure plate surfaces, allowing for smooth engagement and disengagement.

When the clutch begins to engage, the contact pressure between the contact surfaces will increase to a maximum value at the end of the slipping period and will continue to stay steady during the full engagement period. During the slipping period, large amount of heat energy is generated at the contact surfaces, which gets converted to thermal energy by first law of thermodynamics. The heat generated is dissipated by conduction between the clutch components and convection to the environment. Another loading condition is the pressure contact between the contact surfaces that occurs due to the axial force applied the diaphragm spring. In addition to the above output responses, this work also considers the Vibrationa l characteristics of the clutch plate during the full engagement period. The engine and the transmission components experience dynamically varying loads during normal operation. This will cause vibrations and hence, one must design the clutch system so as to avoid resonance with the transmission and engine components as shown by Fang [6].

2. METHODOLOGY

Clutch friction linings are subjected to severe rubbing so that generation of heat in relatively short periods takes place. Therefore, the lining material should have a combination of the following properties to withstand the operating conditions [8]:

- Relatively high coefficient of friction under entire operating conditions.
- Maintenance of friction properties during entire working life.
- Relatively high energy absorption for short periods.
- Withstanding high pressure plate compressive loads.
- Withstanding high impacts of centrifugal force during gear changing.
- Adequate shear strength to transmit engine torque.
- High level of endurance in cyclic working without effecting friction properties.
- Good compatibility with cast iron facings over the entire range of operating temperature.
- A high degree of tolerance against interface contamination without affecting its friction take up and grip characteristics.

Considerations in Designing of a Friction Clutch:

- The following considerations must be kept in mind while designing a friction clutch. The suitable material forming the contact surfaces should be selected.
- The moving parts of the clutch should have low weight in order to minimize the inertia load, especially in high speed service.
- The clutch should not require any external force to maintain contact of the friction surfaces.
- The provision for taking up wear of the contact surfaces must be provided.
- The clutch should have provision for facilitating repairs.
- The clutch should have provision for carrying away the heat generated at the contact surfaces.
- The projecting parts of the clutch should be covered by guard.

Properties of some of commonly used materials for lining of friction surfaces are listed in Table 1.

Table 1: Properties of different materials [9]

Material	Friction Coefficient, f	Maximum Pressure, p_{max} [psi]
Cermet	0.32	*150*
Sintered metal (dry)	*0.29-0.33*	*300-400*
Sintered metal (wet)	*0.06-0.08*	*500*
Rigid molded asbestos (dry)	0.35-0.41	*100*
Rigid molded asbestos (wet)	0.06	*300*
Rigid molded asbestos pads	0.31-0.49	*750*

Rigid molded nonasbestos	0.33-0.63	*100-150*
Semirigid molded asbestos	0.37-0.41	*100*
Flexible molded asbestos	0.39-0.45	*100*
Wound asbestos yarn and wire	0.38	*100*
Wound asbestos yarn and wire	0.38	*100*
Woven cotton	0.47	*100*
Resilien paper (wet)	0.09-0.15	*400*

3. CALCULATIONS

Clutch plate of a Toyota Hilux KUN 25 was selected for sake of analysis. The vehicle has the following specifications:

- Maximum torque   Nm
- Outer diameter mm
- Hub diameter   with 21 splines.

3.1 Torque transmission under uniform pressure

This theory is applicable to new clutches. In new clutches employing a number of springs, the pressure can be assumed as uniformly distributed over the entire surface area of the friction disk. With this assumption, the intensity of pressure between disks,   is regarded as constant.

3.2 Design Calculations

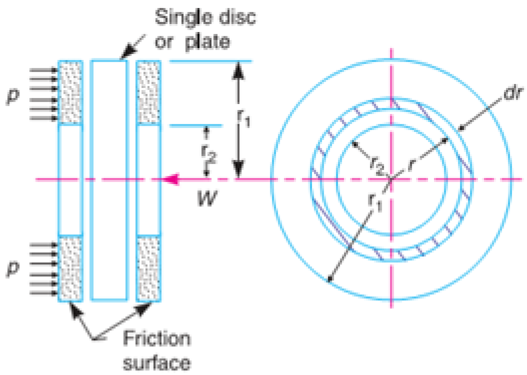

Figure 2. Clutch lining terminology [10]

Various Parameters used for calculations are as follows: (Total axial load of spring),   (External radius of clutch plate),   (internal radius of the clutch plate),   (intensity of pressure between contacting surfaces),   (coefficient of friction between contacting surfaces)
Frictional resistance force offered by ring is given by:

$$F_r = \mu \cdot (2 \cdot \pi \cdot p \cdot r \cdot \delta r) = 2 \cdot \pi \cdot \mu \cdot p \cdot r \cdot \delta r \tag{1}$$

Frictional torque acting on the ring is given as:

$$T_r = F_r \cdot r \tag{2}$$

$$T_r = 2 \cdot \pi \cdot \mu \cdot p \cdot r \cdot \delta r \cdot r = 2 \cdot \pi \cdot \mu \cdot p \cdot r^2 \cdot \delta r \tag{3}$$

This Torque transmitted by single plate clutch is obtained by considering following two assumptions theory.

3.3 Torque transmission under uniform wear

This theory is based on the fact that wear is uniformly distributed over the entire surface area of friction disk. This assumption can be used for worn out clutches/old clutches. The axial wear of the friction disk is proportional to frictional work. The work done by the friction is proportional to the frictional force ($\mu \cdot p$) and the rubbing velocity ($2 \cdot \pi \cdot r \cdot n$) where n is the speed of the disk in revolution per minute.

When the speed n and the coefficient of friction μ are constant for a given configuration, then $Wear\ \alpha\ pr$ [11].

According to this assumption, $p \cdot r = const$.

When the clutch plate is new and rigid, the wear at the outer radius will be more, which will reduce pressure at the outer edge due to rigid pressure plate. This will change pressure distribution. During running condition, the pressure distribution is adjusted such that the product (pr) is constant. Therefore,

$$p \cdot r = p_a \cdot r \tag{4}$$

Where p_a is the pressure at the inner edge of plate, which is also the maximum pressure.

The uniform-pressure theory is applicable only when the friction lining is new. When the friction lining is used over a period of time, wear occurs. Therefore, the major portion of the life of friction lining comes under uniform-wear criterion. Hence, in the design of clutches, the uniform wear theory is used.

The torque transmitting capacity can be increased by three methods:

- Using the friction material with a higher coefficient of friction (μ);
- Increasing the intensity of pressure (p) between disks; and
- Increasing the mean radius of friction disc $\frac{R+r}{2}$.

There are five different materials utilized in modern clutch design [12]:

- “Organic” clutch material, which is a mix of fiberglass and other materials (including brass in some cases) molded or woven into a friction pad.
- Kevlar (and its cousin Twaron), which are synthetic fibers that make for extremely long- lasting (and very forgiving) clutch friction pads.
- Ceramic clutch material, which is mostly a mix of silicon dioxide and various metals and additives, sintered or brazed onto the clutch disc.
- Feramic clutch material, which is fairly similar to ceramic material, except containing a much larger percentage of metal.
- FeramAlloy, which is a new and superior alternative to feramic and ceramic clutch material.

The ratio of inner to outer diameter for maximum torque transmission is given by following equations:

- $X = \frac{D_i}{D_o} = 0.48$ for uniform pressure (5)
- $X = \frac{D_i}{D_o} = 0.577$ for uniform wear (6)

3.4 Calculation for the friction lining based on uniform wear

Baseline data for the calculation of the

$$X = \frac{D_i}{D_o} = 0.577 \text{ for uniform wear}$$

$$D_i = 0.577 \cdot D_o = 0.577 \cdot 260$$

$$D_i = 150\,\text{mm}$$

Outer radius $r_o = 130\,\text{mm}$

Inner radius $r_i = 75\,\text{mm}$

Torque transmission capacity $T = 343\,\text{Nm}$

Effective mean radius $R = \dfrac{r_o + r_i}{2} = \dfrac{130+75}{2} = 102.5\,\text{mm}$

The necessary relationships for the calculation are:

$$T = 2\cdot\mu\cdot W\cdot R$$

$$Normal\ force = 2\pi C\left(r_o - r_i\right)$$

$$W = \pi\cdot p\cdot D_i\cdot\left(D_o - D_i\right)$$

a) Lining mate rial: Asbestos

Coefficient of friction $\mu = 0.35$

$W = 4780.5\ \text{N}$

$p = 0.184\ \text{N/mm}^2$

b) Lining mate rial: Sintered metal

Coefficient of friction $\mu = 0.29$

$W = 5769.5\ \text{N}$

$p = 0.2245\ \text{N/mm}^2$

c) Lining mate rial: Cermet

Coefficient of friction $\mu = 0.4$

$W = 4183\,\text{N}$

$p = 0.1614\ \text{N/mm}^2$

3.5 Calculation for the friction lining based on Uniform pressure

The ratio of inner to outer diameter for maximum torque transmission is:

- $X = \dfrac{D_i}{D_o} = 0.48$ for uniform pressure (7)
- $X = \dfrac{D_i}{D_o} = 0.577$ for uniform wear

$$D_i = 0.48\cdot D_o = 0.48\cdot 260 \quad (8)$$

$$D_i = 124.8\,\text{mm}$$

Baseline data for the calculation of the:

Outer radius $r_o = 130\,\text{mm}$

Inner radius $r_i = 62.4\,\text{mm}$

Torque transmission capacity $T = 343\,\text{Nm}$

$$\text{Effective mean radius } R = \frac{2}{3}\frac{r_o^3 - r_i^3}{r_o^2 - r_i^2} = \frac{2}{3}\frac{130^3 - 62.4^3}{130^2 - 62.4^2} = 100.16 \text{ mm}$$

The necessary relationships for the calculation are:

$$\text{Torque transmission capacity (T): } Torque = n \cdot \mu \cdot W \cdot R$$

$$W = \pi \cdot p \cdot \left(r_o^2 - r_i^2\right)$$

a) Lining mate rial: Asbestos

$$\text{Coefficient of friction } \mu = 0.35$$
$$W = 9784.3 \text{ N}$$
$$p = 0.1145 \text{ N/mm}^2$$

b) Lining mate rial: Sintered metal

$$\text{Coefficient of friction } \mu = 0.29$$
$$W = 5904.43 \text{ N}$$
$$p = 0.1445 \text{ N/mm}^2$$

c) Lining mate rial: Cermet

$$\text{Coefficient of friction } \mu = 0.32$$
$$W = 5350.815 \text{ N}$$
$$p = 0.131 \text{ N/mm}^2$$

d) Lining mate rial: Ceramic

$$\text{Coefficient of friction } \mu = 0.4$$
$$W = 4280.65 \text{ N}$$
$$p = 0.1045 \text{ N/mm}^2$$

Table 2: Propert Comparison of lining materials with uniform wear and uniform pressure

Materials	Uniform wear		Uniform pressure	
	Axial force, [N]	Pressure, [N/mm^2]	Axial force, [N]	Pressure, [N/mm^2]
Asbestos	4780.5	0.184	4892.5	0.1145
Sintered	5769.5	0.2245	5904.43	0.1445
Cermet	5228.5	0.2015	5350.81	0.131
Ceramic	4183	0.1614	4280.65	0.1045

4. FEA ANALYSIS

The finite element analysis is the most widely accepted computational tool in engineering analysis [13]. Through solid modelling, the component is described to the computer and this description affords sufficient geometric data for construction of mesh for finite element modelling. In this project the clutch plate assembly using different lining materials was designed in the previous chapter. In this chapter finite element analysis is going to be done using Ansys software. In the following subchapters structural and thermal analysis is going to be done for each clutch assembly parts and compare different lining to choose the best lining, which were designed in the previous part. 3D modelling was done using Catia V5 for each plate assembly parts and now we are going to import those models to Ansys to do static structural analysis.

Table 3: Propert Comparison of lining materials with uniform wear and uniform pressure

Materials	Tensile yield strength [MPa]	Calculated *p* [N/mm^2]	Poisson ratio [-]	Modulus of elasticity [GPa]	Density [kg/m^3]
Asbestos	800	0.184	0.28	165	2800
Sintered metal	140	0.2245	0.24	115	6400
Cermet	1039	0.2015	0.23	380	5000
Ceramic	1138	0.1614	0.22	325	2130
Kevlar	3240	0.184	0.36	71	1470
Spring steel	1000		0.273	210	7861
Cast ion alloy ASTM A220	130		0.28	110	7200

4.1 Clutch plate assembly with asbestos lining

Clutch disk shown in Figure 3, in the form of finite elements mash.

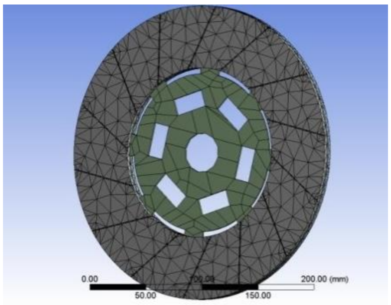

Figure 3. Meshed clutch disc

Material property and geometry da ta were defined (as per Table 3). The Environment (a combination of loads and supports) was defined as follows:

- Moment: 171.5 Nm (each side)
- Pressure: 0.184 Mpa.

The Model was submitted to the ANSYS solver and the solutions for the Equivalent von-Mises stress, Total Deformation and Stress Tool were obtained. Figure 4 shows the distribution of equivalent von-Mises stress over the clutch plate. Figure 5 shows the distribution of total deformation over the clutch plate. Figure 6 shows the distribution of Factor of Safety (Stress Tool) over the clutch plate.

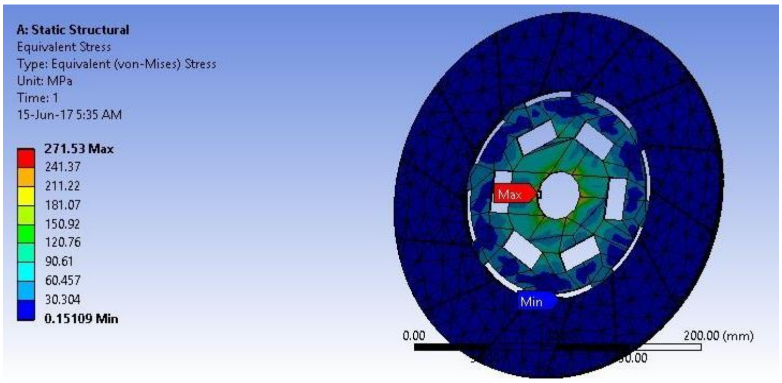

Figure 4. The equivalent von-Mises stress plot for the clutch plate

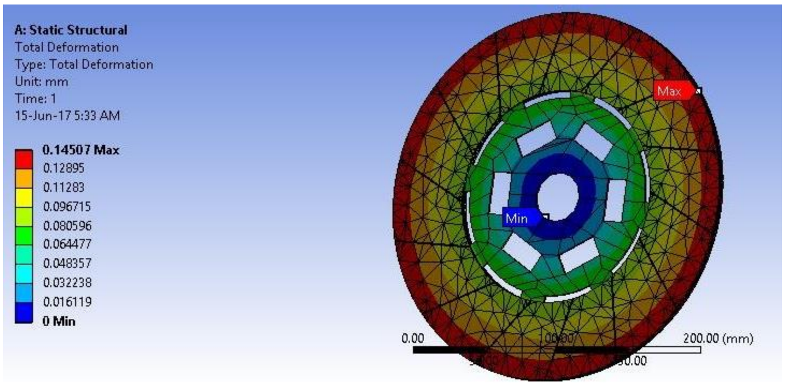

Figure 5. The Total Deformation plot for the clutch plate

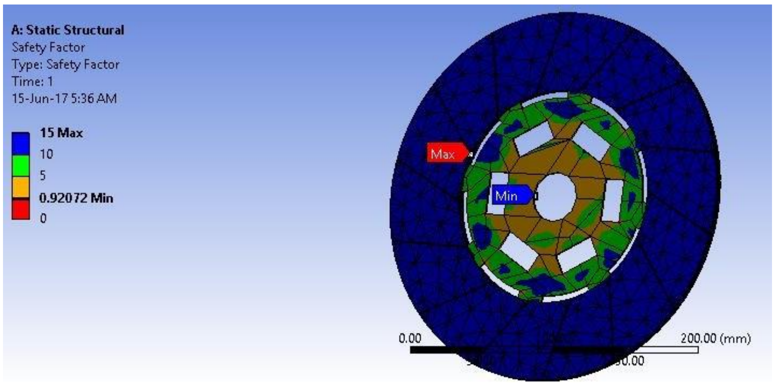

Figure 6. The Factor of Safety (Stress Tool) plot for the clutch plate

4.2 Clutch plate assembly with sintered metal

A Mesh was created (Dividing the model into small elements). Material property and geometry data were defined (as per Table 3). The Environment (a combination of loads and supports) was defined as follows:

- Moment: 171.5 Nm (each side)
- Pressure: 0.2245 Mpa.

The Model was submitted to the ANSYS solver and the solutions for the Equivalent von-Mises stress, total Deformation and Stress Tool were obtained as seen in Figure 7−9.

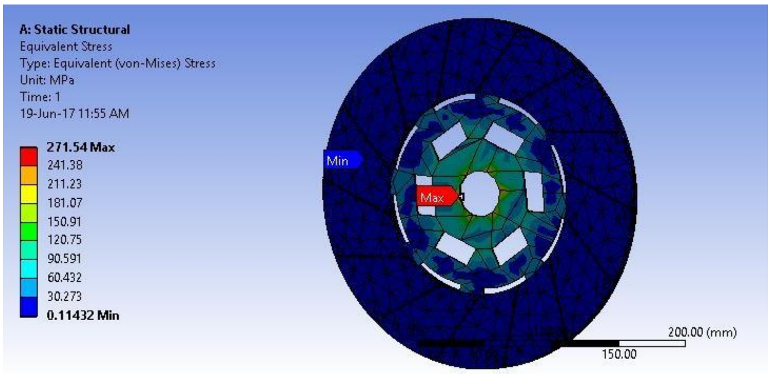

Figure 7. The equivalent von-Mises stress plot for the clutch plate

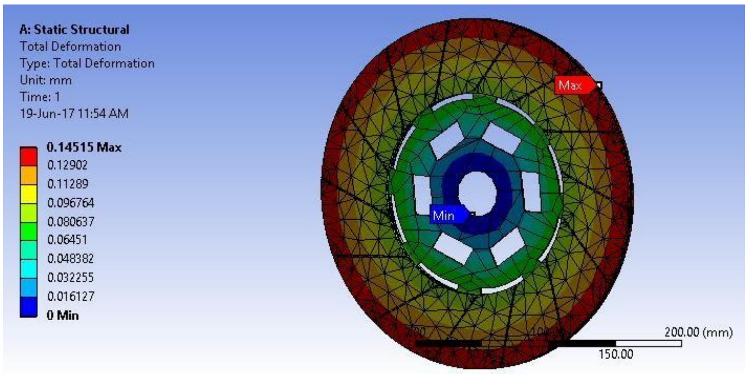

Figure 8. The Total Deformation plot for the clutch plate

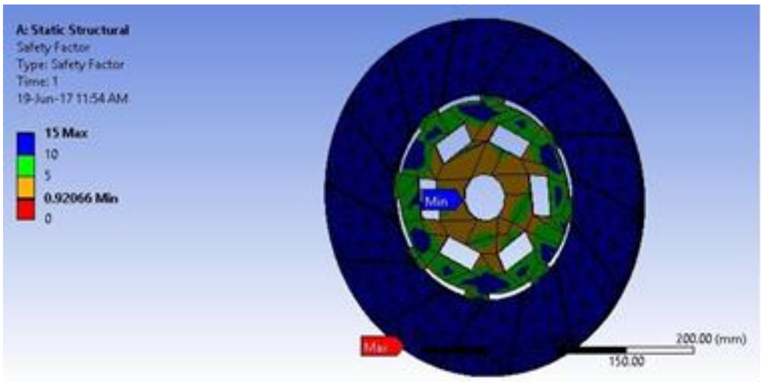

Figure 9. The Factor of Safety (Stress Tool) plot for the clutch plate

4.3 Clutch plate assembly with cermet

A Mesh was created (Dividing the model into small elements). Material property and geometry data were defined. The Environment (a combination of loads and supports) was defined as follows:

- Moment: 171.5 Nm (each side)
- Pressure: 0.2015 Mpa.

Obtained results are shown on Figures 10-12.

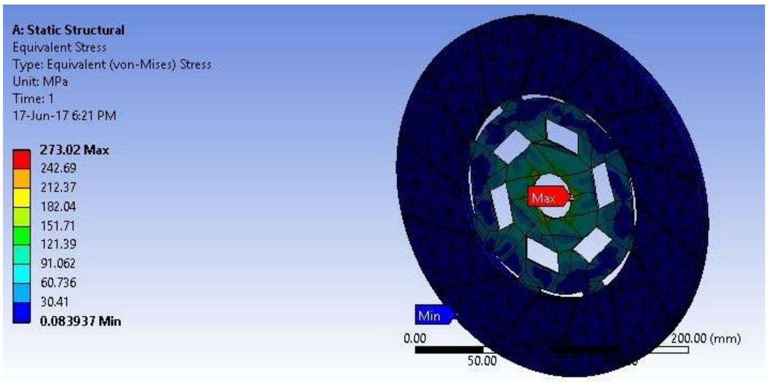

Figure 10. The equivalent von-Mises stress plot for the clutch plate

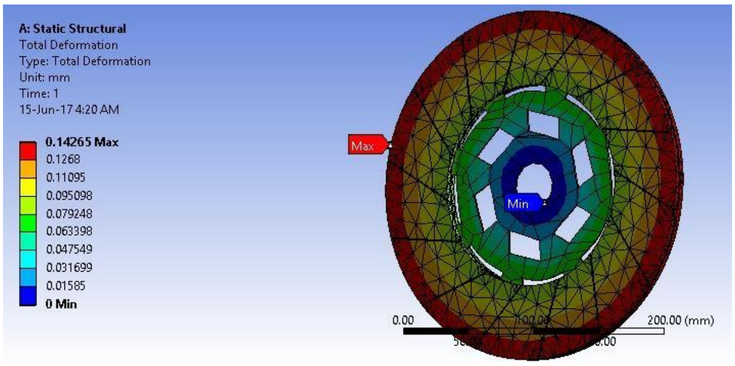

Figure 11. The Total Deformation plot for the clutch plate

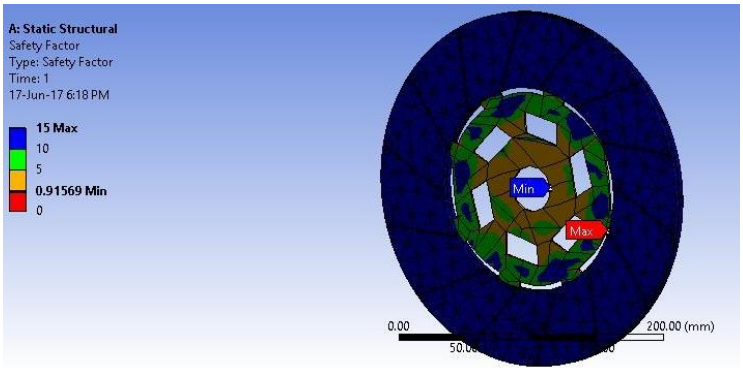

Figure 12. The Factor of Safety (Stress Tool) plot for the clutch plate

4.4 Clutch plate assembly with ceramic

A Mesh was created (Dividing the model into small elements). Material property and geometry data were defined. The Environment (a combination of loads and supports) was defined as follows:

- Moment: 171.5 Nm (each side)
- Pressure: 0.1614 Mpa.

Obtained results are shown on Figures 13-15.

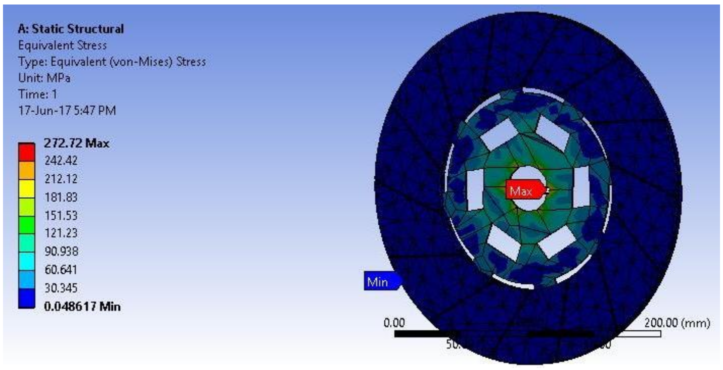

Figure 13. The equivalent von-Mises stress plot for the clutch plate

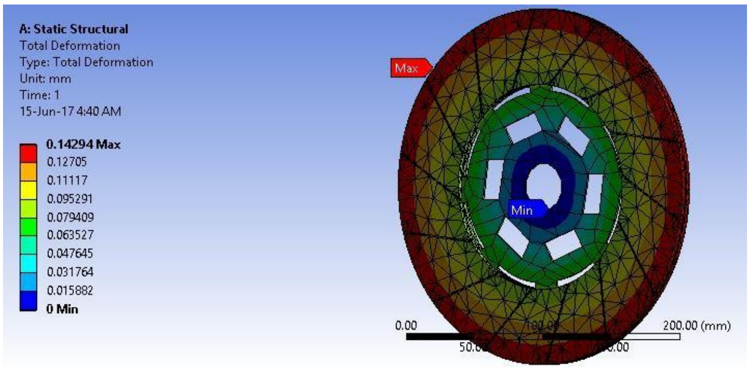

Figure 14. The Total Deformation plot for the clutch plate

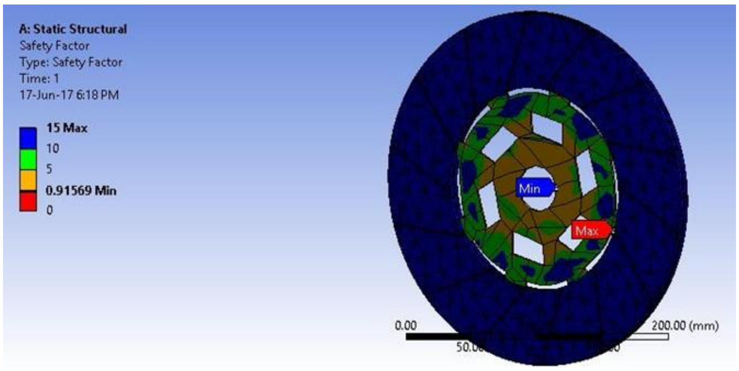

Figure 15. The Factor of Safety (Stress Tool) plot for the clutch plate

5. CONCLUSIONS

In this work, clutch plate of an automotive clutch assembly has been designed using different materials and simulated using ANSYS software for comparison. Among those different lining materials cermet friction material was selected. Generated Heat between friction disk and flywheel, which is the main reason for clutch wear can be minimized by selecting suitable material. A good contact pressure also reduces wear during slippage time.

REFERENCES

[1] Narayan S., Effects of Various Parameters on Piston Secondary Motion, SAE Technical Papers, 2015, 2015-01-0079, doi: https://doi.org/10.4271/2015-01-0079.

[2] A&C Automotive, Internet address: http://www.acautomotive1.co.uk/clutches.php, accessed 10.03.2018.

[3] Narayan S., A review of diesel engine acoustics, FME Transactions, 2014, 42(2), 150-154, doi: 10.5937/fmet1402150N.

[4] Narayan S., Correlation between cylinder pressure and noise emissions from diesel engine, Journal of KONES Powertrain and Transport, 2015, 22(1), 243-254, doi: 10.5604/12314005.1161775.

[5] Buzzoni M., Mucchi E., G. Dalpiaz, A CWT-based methodology for piston slap experimental characterization. Mechanical Systems and Signal Processing, 2017, 86(3), 16-28, doi: 10.1016/j.ymssp.2016.10.005.

[6] Fang C., Xianghui M., Youbai X., A piston tribodynamic model with deterministic consideration of skirt surface grooves. Tribology International, 2017, 110, 232-251, doi: 10.1016/j.triboint.2017.02.026.

[7] Zhao B., Cui Y., Xie Y., Zhou K., Dynamics and lubrication analyses of a planar multibody system with multiple lubricated joints. Proceedings of the Institution of Mechanical Engineers, Part J: Journal of Engineering Tribology, 2017, 12, 47-74, doi: 10.1177/1350650117713891.

[8] Angel World Zone, Internet address: http://angelworldzone.com/Two%20wheeler%20Dynamics14_1.html, accessed 10.03.2018.

[9] Budynas R., Nisbett K., Shigley's Mechanical Engineering Design (McGraw-Hill Series in Mechanical Engineering) 10th Edition, 2014, ISBN 978-0073398204.

[10] University Of Al-Qadisiyah, Internet address: http://qu.edu.iq/el/pluginfile.php/32610/mod_resource/content/1/Clutch.pdf, accessed 10.03.2018.

[11] NPTEL, Internet address: http://www.nptel.ac.in/courses/116102012/clutches/single%20friction%20disk%20clutch.html, accessed 28.02.2018.

[12] Quora, Internet address: https://www.quora.com/What-is-the-material-used-for-making-clutch-plates, accessed 28.02.2018.

[13] Stojanovic N., Glisovic J., Structural and thermal analysis of heavy vehicles' disc brakes, Mobility & Vehicle Mechanics, 2016, 42(1), 9-16, ISSN 1450-5304.

MOBILITY & VEHICLE MECHANICS

DOI: 10.24874/mvm.2018.44.01.03
UDC: 539.379(086.48)

ESTIMATION OF EES VALUES BY VEHICLE 3-D MODELLING

Zoran Papić [1], Vuk Bogdanović [2], Goran Štetin [3], Nenad Saulić [4]*

Received: November 2017 Revised: December 2017 Accepted: January 2018

RESEARCH ARTICLE

ABSTRACT: Energy Equivalent Speed value (EES) is the base of energy method for crash velocity assessment. Estimation of EES value is based on deformation depth and a vehicle stiffness coefficient. Vehicles that are damaged in traffic accidents are usually unavailable for accidents experts so they have to rely on photographs of those vehicles. Development of 3-D photogrammetry and leading software solutions in the field of photogrammetry allowed more detailed overview of deformation on vehicles that were involved in accidents. One of those software solution, that provide 3D models from pictures taken in the planned photo session, is PhotoModeler Scanner. By comparing 3D models of a damaged and undamaged vehicle, experts can get more insight into the type and damage intensity. Analysing those 3D models, information about deformation depth are obtained. This paper shows the procedure of forming a 3D model of an undamaged vehicle created from photographs that were taken in the planned photo session and processed in PhotoModeler Scanner software. This model was compared with a 3D model of the same type of vehicle made from photographs taken at the accident spot. Based on measurements that are taken from those 3D models, the main elements for EES estimation are determined.

KEY WORDS: EES, PhotoModeler, 3-D model, deformation

PROCENA EES VREDNOSTI TRODIMENZIONALNIM MODELIRANJEM VOZILA

REZIME: Vrednost brzine ekvivalentne energije (EES) je osnova energijskog metoda za procenu brzine udara. Procena EES vrednosti je zasnovana na dubini deformacije i koeficijentu krutosti vozila. Vozila koja su oštećena u saobraćajnim nezgodama obično nisu dostupna stručnjacima za nezgode, pa se oni moraju osloniti na fotografije tih vozila. Razvoj 3D fotogrametrije i vodećih softverskh rešenja iz oblasti fotogrametrije omogućio je detaljni prikaz defomacije na vozilima koja su bila uključena u nezgode. Jedno od tih softverskih rešenja, koje pružaju 3D modele sa slika snimljenih tokom planiranje foto sesije, je PhotoModeler Scanner. Poredeći 3D modele oštećenih i neoštećenih vozila, stručnjaci mogu imati više uvida u tip i intezitet štete. Analizirajući ove 3D modele, dobijene su informacije o dubini deformacije.

[1] *Zoran Papić, Ph.D., prof., University of Novi Sad, Faculty of Technical Sciences, Department of Traffic Engineering, Trg Dositeja Obradovića 6, 21000 Novi Sad, Serbia, njele@uns.ac.rs, (*Corresponding author)*
[2] *Vuk Bogdanović, Ph.D., prof., University of Novi Sad, Faculty of Technical Sciences, Department of Traffic Engineering, Trg Dositeja Obradovića 6, 21000 Novi Sad, Serbia, vuk@uns.ac.rs*
[3] *Goran Štetin, Ph.D. student., University of Novi Sad, Faculty of Technical Sciences, Department of Traffic Engineering, Trg Dositeja Obradovića 6, 21000 Novi Sad, Serbia, stetinns@gmail.com*
[4] *Nenad Saulić, M.Sc., assist., University of Novi Sad, Faculty of Technical Sciences, Department of Traffic Engineering, Trg Dositeja Obradovića 6, 21000 Novi Sad, Serbia, nenadsaulic@gmail.com*

Ovaj rad pokazuje proceduru formiranja 3D modela neoštećenog vozila od fotografija snimljenih na planiranoj fotosesiji obradjenih u PhotoModeler Scanner softveru. Ovaj model je upoređen sa 3D modelom istog tipa vozila napravljenog od fotografija snimljenim na mestu nezgode. Na osnovu merenja koja se uzimaju od tih 3D modela, odredjeni su glavni elementi za procenu EES-a.

KLJUČNE REČI: EES, PhotoModeler, 3-D model, deformacija

ESTIMATION OF EES VALUES BY VEHICLE 3-D MODELLING

Zoran Papić, Vuk Bogdanović, Goran Štetin, Nenad Saulić

1. INTRODUCTION

Basis for efficient and reliable reconstruction of every traffic accident is documentation compiled during car accident investigation. Photograph of the site of the accident is an integral part of investigation documentation, by which, in the most objective way, the information related to the place of an accident, involved objects and subjects can be collected and transferred. Due to the technology development, a photograph has become a source of a great number of information. In other words, a photograph has become irreplaceable in many aspects of people's lives, in which it is not only used for documentation purposes, but also as a part of a technological process. Using a photograph for measuring purposes is an example where its documentation quality is put into background, and primary use is for its geometric quality. Scientific discipline that deals with photograph usage for measuring purposes is called photogrammetry. This refers to a measuring method by which position, dimension, and shape of a recorded detail is reconstructed using one or more photographs, without direct contact with them. One of the main photogrammetry tasks is measurement of individual points, that is determining point position in two-dimensional or three-dimensional space using photographs. Today, photogrammetry is used in different fields. The widest usage has found in geodesy and architecture for the purposes of terrain and object surveying. With the improvement of measuring tools, the photogrammetry accuracy is becoming even bigger, so today it is also used in industry during production of complex models and it reaches accuracy from 0.01 mm.

With the introduction of computer technology, photogrammetry is more economic and efficient. Photographs can easily be transferred between devices, and by additional software tools the process of photogrammetry analysis is considerably simplified, more automatic and faster. Due to its numerous advantages, photogrammetry is more and more applied in forensic engineering. Using photogrammetry at a scene investigation process, time investigation is considerably shorter and what is avoided are the mistakes that can occur due to subjective oversight or current inability to find and identify all the clues that can be used in further event analysis. Photogrammetry recording of accident scene and vehicles involved in the accident provides a permanent archive recording, based on which all future measurements could be done, for the purposes of determining dynamic parameters of the accident, finding new clues and evidences, etc.

Deformation on the vehicle caused by a collision represents safe and reliable data which can be used when making conclusions regarding clarifying the circumstances at which the traffic accident occurred. If the damaged vehicle is photographed properly, information about its deformations will be available for a long time, and by applying photogrammetry very usable. Based on a 3D vehicle model made by photogrammetry recording measurements can be done of individual characteristic points on a vehicle and, if needed, do model orientation and use it for:

- measuring the depth of vehicle damage
- calculation of vehicle energy lost on deformed work in collision process
- determining collision speed of a vehicle
- determining collision position of a vehicle
- determining movement direction of vehicles before collision, etc.

Experts who are dealing with traffic accident reconstruction, are most often available only photographs recorded during the site accident investigation, at which, depending on the circumstances during the investigation and equipped personnel who did it, are shown damaged parts on a vehicle, with more or less details. Due to numerous limitations at scene investigation process, number of vehicle photographs involved in the accident is usually not enough to form a detailed 3D model, but it is quite sufficient for damage analysis on it. On the other hand, it is much easier to make a 3D model of an undamaged vehicle, of the same type as the vehicle that had been in a traffic accident, when there are no limitations regarding number of photographs and angles of recordings. This way, it is possible to do an overlap of contours of undamaged parts on both vehicles, while the damage of a vehicle that had been in an accident will be clearly visible.

2. THE BASIS OF 3D PHOTOGRAMMETRY

Getting necessary geometric information about recorded terrain can be done by measuring one tape of recorded terrain (or object). Considering that at two-dimensional objects all points lie in one plane, reconstruction of that object would be possible based on only one photograph, with the knowledge of referent length visible on them. This is done by copying planes of copied object into a picture plane, in other words, by transforming its perspective into a perspective of a strictly vertical recording.

3D photogrammetry is applied when it is necessary to reconstruct an object in three-dimensional system, meaning to perform a recovery of information lost in a process of recording. Photograph represents two-dimensional image of three-dimensional objects, therefore in process of its making the third dimension of photographed object is being lost. Therefore, the lost information in the photograph is actually the third dimension. Transformation into 3D recording is done by recovering information lost in the process of recording, i.e. by determining from which exact position along the trajectory of caught ray the information was received. To have a three-dimensional insight in a photographed object, the photograph must be composed from at least two different positions, where recordings must include the same parts of objects that are visible on them, but from different angles and perspectives

(Figure 1).

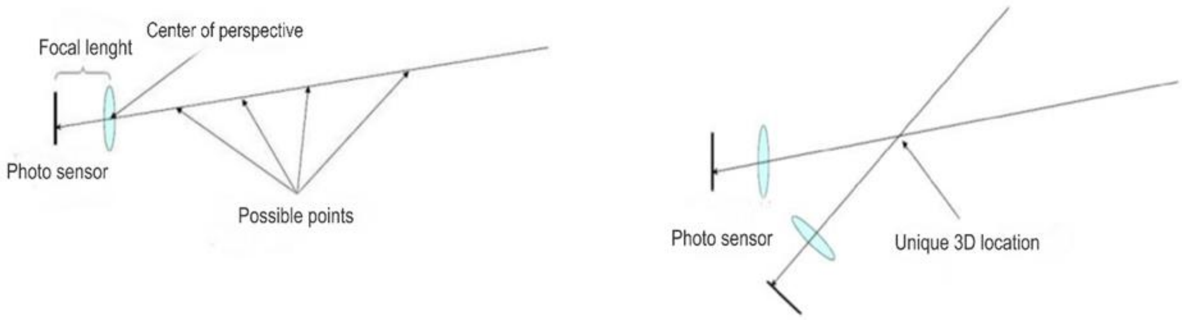

Figure 1. Determining the unique 3D location point-space

Geometric relations between photographs are established by mathematical principals of determining coordinate points of recorded objects. Without computer technology, it is very difficult to provide production of precise stereo photograph couples. Modern software in photogrammetry field provides finding 3D coordinate object points in space using points coordinates projection of an object on the photograph plane, all this is done using two photographs by choice of the same object. During the marking of mutual object points on the photograph plane, an error can occur that can influence the precision of measurement or object modeling. This problem is solved by recording the coordinate points in space using more photographs, so that the precision of the process is bigger.

3. THREE-DIMENSIONAL MODELING USING PHOTOMODELER PACKAGE PROGRAM

Photomodeler Scanner is currently among top three best software solutions whose primary purpose is photogrammetric process of recordings and creation of 2D and 3D models. The software itself is created in that way that due to a high level of automation, which is not the case with previous programs, covers the needs of aero as well as the close-range recording of terrain and objects.

Information gathering at a terrain must satisfy basic principals of photogrammetric recording with which is ensured the necessary level of accuracy that in well-calibrated projects is measured in millimeters. This level of accuracy, though desirable, is not necessary when photogrammetric video rectification is done, however it is of great significance during the determination of depth of vehicle damage through photogrammetry of the given 3D model. Camera calibration, by which the information gathering is done, has a crucial role when it comes to the amount of achieved accuracy. Photomodeler in its data base contains a large number of basic parameters for cameras from various manufacturers so that it can recognize with what camera the recording had been done, apart from that, calibration is necessary for parameter characterization specific for every individual camera. Parameters for camera calibration are the following:

- sensor specification
- pixel size in millimeters
- focal length[48]
- radial curving of camera lenses
- distortion due to non-centric camera elements
- linear distortion.

Calibration is done according to established procedure that can be found in the Photomodeler manual package and it is not different than standard calibration procedures in any other software for the same purpose.

It is desirable that recording area during calibration has similar size as future calibration projects so that manually set focal length is the same, with which the level of accuracy is enhanced.

When the calibration is successfully done, a good basis is formed for the high level of project accuracy. Practical use of Photomodeler Scanner, unlike standard Photomodeler package, as well as the other software solutions in this field is portrayed in the high level of process automation when determining unique 3D point positions in space. When generating 3D model of a object or item, basically it is necessary to make as many photographs as possible from different positions, and photograph selection with a good angle of overlap can be done during later work. If for some reason there are not enough photographs to start automatic orientation (in reality this is less than 4 recordings) or it is not possible from another reason, as a possibility there is manual connecting of points in space and then photographs should be chosen according to this principle:

- Make sure that the distance between two positions of camera when taking pictures is at least 10-20% (or more) from the average distance between referent points. This is an important principle for the first two photographs at which orientation is done
- Make sure that referent points, which are used for orientation, are spread out in two directions, or even better, if possible, in three directions. Relative orientation will be done easier if referent points do not lie in one area
- One should bear in mind that the bigger angle of intersection between two or more rays the coordinates (XYZ) will be determined better
- Where possible, one should make sure that referent object points fulfill as bigger picture format as possible. This will increase precision and reliability of relative orientation
- One should always decide to have more referent points. Even though in theory there should be 5 points per photograph minimum (during stereo orientation), appropriate number should not be less than 12, if we want to be sure that photogrammetry orientation will work
- Not all referent points have to be present in all photographs but they have to be present in enough photographs.

If the previous principles are respected, project will be successfully oriented manually. For automation orientation, apart from above mentioned, one should pay attention to the following as well:

- avoid surfaces at which there is no texture
- avoid moving scenes; object must be in focus
- avoid reflection (common problem when photographing vehicles).

Using Automated Point Clouds & SmartMatch options, automation orientation of a video is done and characteristic points are assigned to project (Figure 2 and 3).

Figure 2 and 3. Undamaged vehicle and generated cloud points with camera positions at the moment of recording

The project is oriented in photogrammetry sense which means that camera positions are determined at the moment of recording as well as the positions of characteristic points. Further process of connecting and model forming is done by automation generating of thick point cloud DanseSurface, and then manually, outlining vehicle contours based on the points on it, so that the measurement of damage depth is done following the contours.


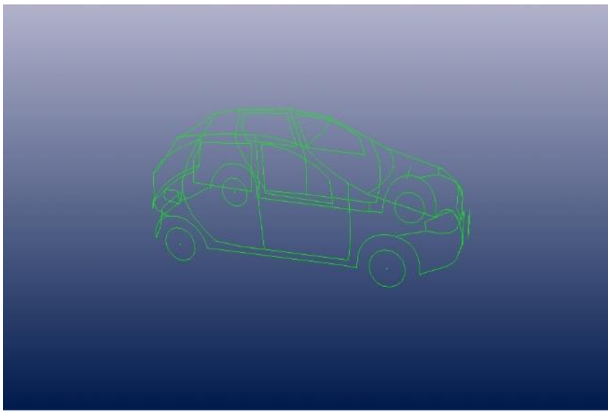

Figure 4 and 5. 3D model made by DanseSurface option and connecting points at vehicle contours

The same generating model process is applied on the photographs of a damaged vehicle that are gathered in the field. In the project are used photographs of a damaged vehicle made by auto service, right before vehicle repair. Considering that the damaged vehicle no longer exists, these photographs are the only source of information about damage depth.


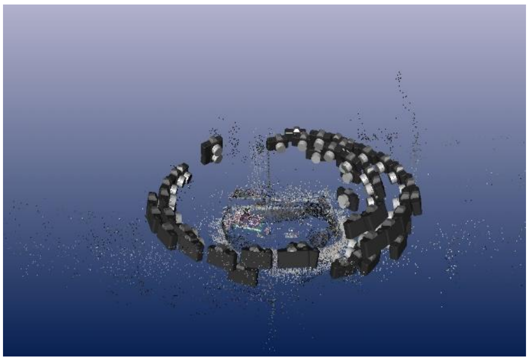

Figure 6 and 7. Damaged vehicle and generated point cloud with camera positions at the moment of recording

Finished model is shown in the next Figure.

Figure 8. 3D model with DanseSurface option

In this occasion, making the 3D model based on the damaged vehicle contours is not done because that process takes up a lot of time, and since undamaged parts of the damaged vehicle completely suit undamaged vehicle based on geometrics, this is not necessary.

Measurements acquired from photographs of damaged vehicle will be paired (connected) with undamaged parts of given damaged vehicle. As already mentioned, these damaged parts represent the carriers of precise vehicle geometrics and therefore it is clear why exactly these parts are used in the process of matching. After creating a 3D model of damaged vehicle and matching mutual points of two models, damages on the vehicle are clearly shown by comparing 3D model contours.

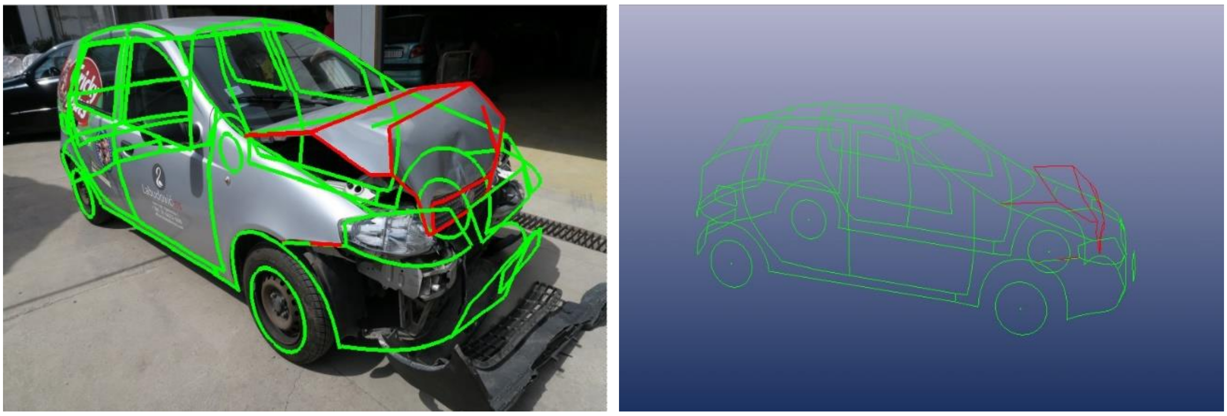

Figure 9 and 10. Removing contours of damaged and undamaged vehicle

Figure 9 shows how undamaged vehicle fits into geometrics of undamaged vehicle parts that had been involved in a traffic accident. It is clearly visible that contours of undamaged parts almost perfectly fit together, and all deviations of these two models are concentrated at the front part, i.e. are formed as a result of deformation in the process of a collision. By measuring deviations in contours of 3D model of damaged and undamaged vehicle at the front part, average front part deformation is set to be around 0.15 m.

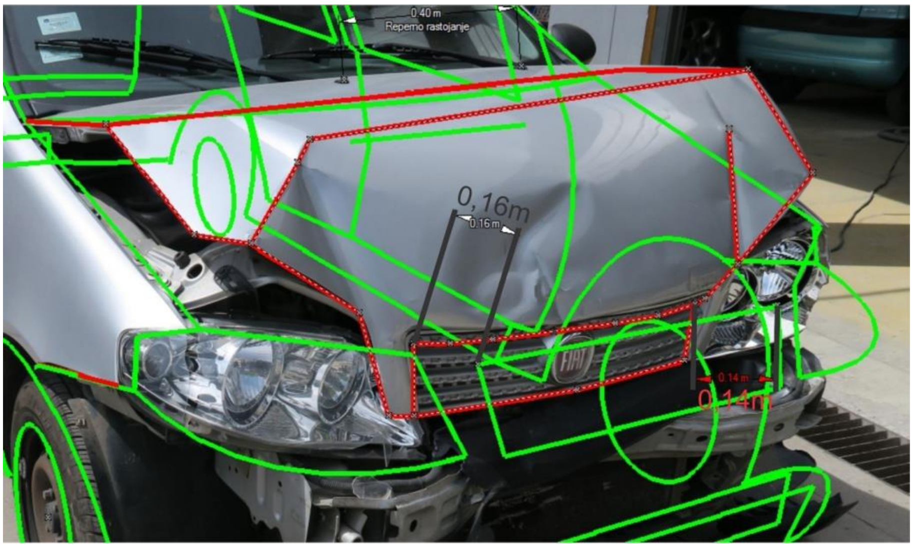

Figure 11. Damage depth

4. DETERMINING EES VALUES APPLYING PC CRASH PACKAGE PROGRAM

The deformation energy, i.e. the energy consumed during the complex process of a vehicle collision for the structure deformation, is of utmost importance for both passive and active safety. It is also a basis for the calculation of kinematic and dynamic parameters of the vehicle, determined during the retrospective research of road events.

The deformation magnitude determines the deformation energy, taking into consideration the vehicle's design parameters expressed by the stiffness coefficients.

The profilometer method is the classical method for determining the deformation magnitude, and it uses a Cartesian coordinate system. Furthermore, new methods based on photographic technique have been developed, such as the PhotoModeler method.

4.1 Car deformations and the deforming energy

In the majority of cases, one of the main goals of reconstruction of road accidents is the determination of vehicle speed prior to collision. Main methods used for approaching the road accidents reconstruction are: impulse method, based on the laws of conservation of the linear and angular impulse and the deformation method based on the laws of conservation of the linear impulse, angular impulse and energy.

The use of the deformation method implies the adoption or existence of certain models of deformation which express the connection between the deformation magnitude and the collision normal force per unit width of the deformed area. The deformation models can be either static or dynamic. The determination of deformation energy for the dynamic deformation models is done based on the dynamic deformations, while the static models use the magnitude of the remnant static deformations for calculating the deformation energy. In contrast to the dynamic models which express the relationship between force and dynamic deformation of the vehicle body, the static models are showing the relationship between force and the plastic remnant deformation of the vehicle, assimilating this dependence as linear.

It can be concluded that determining the total kinetic energy consumed during the impact is done based on the deformation of the vehicle constructive elements, in particular the car body elements. In order to measure the vehicle's deformations, the magnitude of these deformations in several points of the deformed area needs to be determined. The energy consumed for the deformation of the vehicle constructive structure during the impact may be determined on the basis of the remnant deformation of the car body elements, using the vehicle's stiffness coefficients specific to the deformed area.

The PC Crash software uses the following relation in order to calculate the deformation energy.

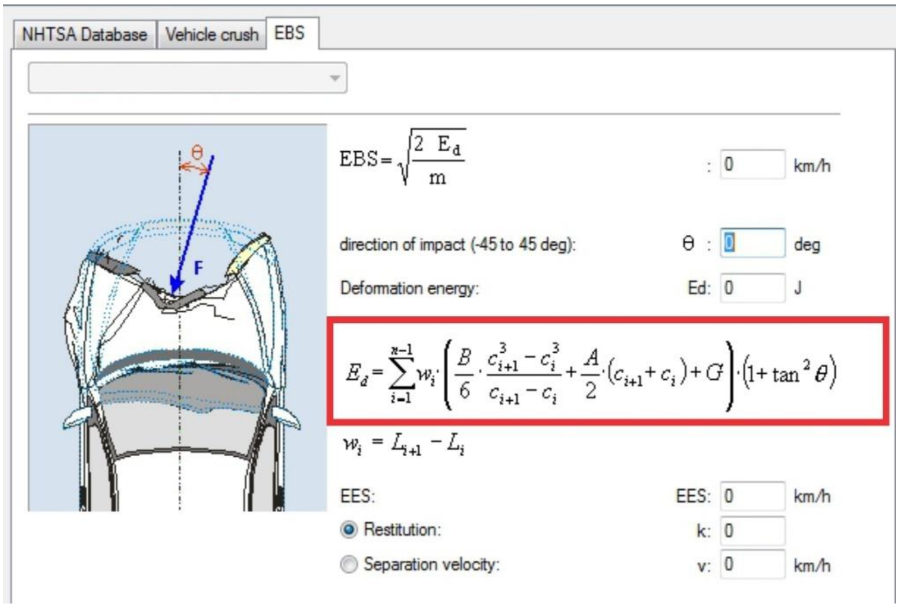

$$E_d = \sum_{i=1}^{n-1} w_i \cdot \left(\frac{B}{6} \cdot \frac{c_{i+1}^3 - c_i^3}{c_{i+1} - c_i} + \frac{A}{2} \cdot (c_{i+1} + c_i) + G \right) \cdot (1 + \tan^2 \theta)$$

$$w_i = L_{i+1} - L_i$$

Figure 12. Relation used to calculate the deformation energy in the PC Crash software

where:

E_d - deformation energy (J);

A, B, G – stiffness coefficients;

C_i, C_i+1 – the deformation measured at point i and point i+1 (m);

L_i, L_i+1 – the rate of the measuring station from point i, and point i+1 (m);

w_i – the distance between two consecutive measuring stations (m);

Θ – angle between the longitudinal axis of the vehicle and the direction of the main impact force (degree).

The deformation energy thus calculated corresponds to the remanent deformation. The car body dynamic deformation reaches the maximum value at the impulse point during compression. Afterwards, during the restitution phase, the deformation magnitude is decreased to the static deformation value.

5. CALCULATION EBS VALUES IN CRASH3 STANDARD

Determining EBS values in PC-Crash program package is done through CRASH3 (Computer Reconstruction of Accident Speeds on the Highway) program that is implemented in PC Crash.

The assumptions of standard CRASH3 are as follows. Cars were generally divided into mini, sub-compact, compact, intermediate, and full-size, excluding trucks and buses. Currently, databases are being extended with pick-up and van vehicle types. Three impact directions are distinguished: front, side, and rear, assuming that body stiffness structure in these areas is uniform. Taking into consideration all unavoidable errors at a particular analysis stage, such simplification is acceptable, nevertheless, the analysis of accident mechanics has to be done in a wide field of tolerance.

Measurement of deformation profile has been standardized by NHTSA and is described in NASS protocol (National Accident Sampling System (71)).

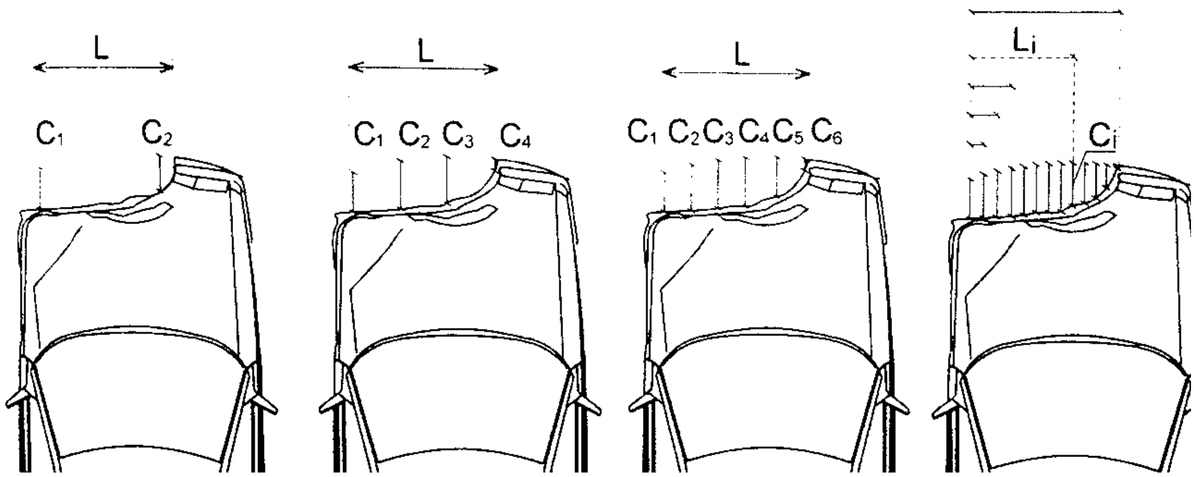

Figure 13. Measurement of vehicle deformation profile

1. Deformation width measure L.
2. Divide length L into several sequences and in these points measure deformation depth in direction perpendicular to vehicle front, side or rear surfaces, regardless of impact force displacement direction. Most frequently, six points are selected, traditionally called C_1-C_6 and this is how data from crash tests are usually given.
3. Depth measurement refers to deformation profile (i.e. so-called contact delmageformation), rather than the total range of induced deformations.
4. Perform measurement parallel to roadway plane.
5. Additionally, measure impact force angular displacement of vehicle longitudinal or lateral axis.

6. CALCULATION EBS VALUES

The contact deformation profile of Fiat Punto was measured in six points. Since the damage is considerable, we can adopt a simplifying assumption that EBS≈EES.

The contact deformation profile of Fiat Punto was measured in six points. Since the damage is considerable, we can adopt a simplifying assumption that EBS≈EES.

Parameters that provide figures in the EBS calculation (stiffness parameters of vehicle A and B) are calculated based on the data acquired by crash tests.These data for given vehicle can be found in NHTSA data base that is listed by manufacturers and vehicle models in the first tab Crash 3 EBS Calculation window. If a vehicle for which we want to do EBS calculation values is not found in the mentioned data base, we can enter stiffness parameters of a vehicle manually, if they are familiar to us, or, what is also the recommendation of PC-CRASH software manufacturer, we can take a benchmark vehicle of similar characteristics. During the selection of a benchmark vehicle, based on which stiffness coefficient will be determined, damage at a front part of tested vehicle must be taken into account to match the damages of our vehicle, i.e. that the damages' width and depth are approximately equal. Since in the NHTSA database are no data for the vehicle Fiat Punto, during EBS calculations values, as a benchmark vehicle is taken Ford Fiesta.

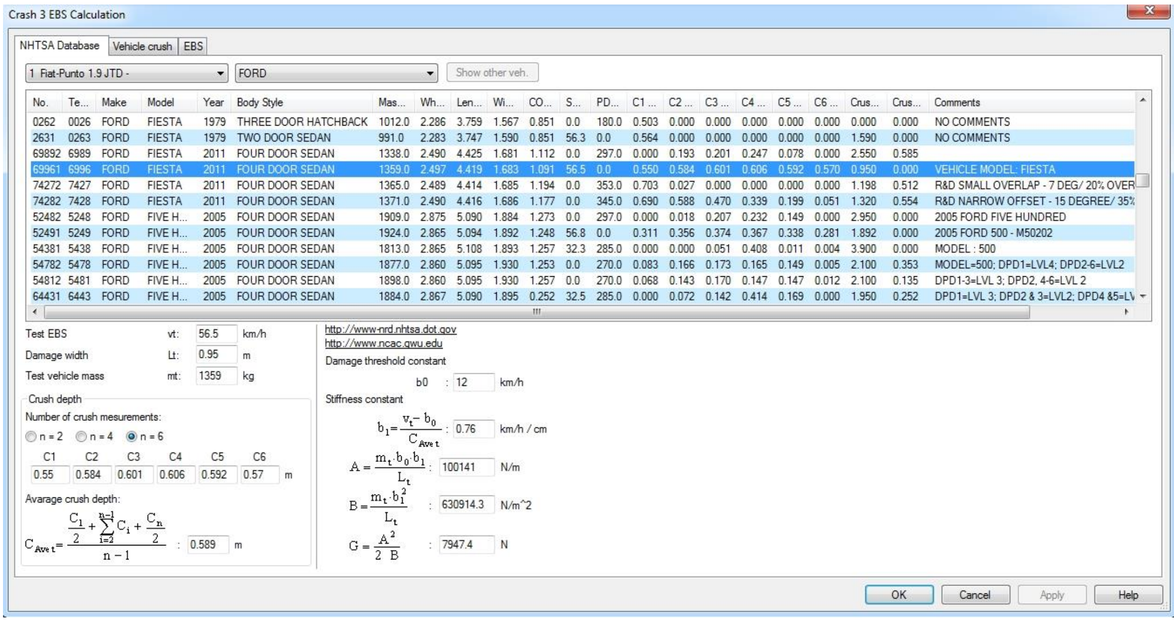

Figure 14. Choosing Crash test and benchmark vehicle

When crash test, which by characteristics and vehicle type matches our vehicle (or if crash test parameters are entered manually: impact velocity V_t, deformation width L_t, vehicle mass m_t, contact deformation profile and permanent deformation boundary velocity b_0), is chosen, i.e. when we have relevant parameters of vehicle stiffness, we can move on to defining the measured depth of our damaged vehicle in Vehicle crash tab. Here is firstly important to determine based on how many points the damaged depth is measured, the depth of every point, as well as its distance in relation to the front left vehicle angle, i.e. point C_1. In our case, measuring had been done based on six points along the front part of the vehicle. Measures and point positions at the measuring moment are given in the next Figure.

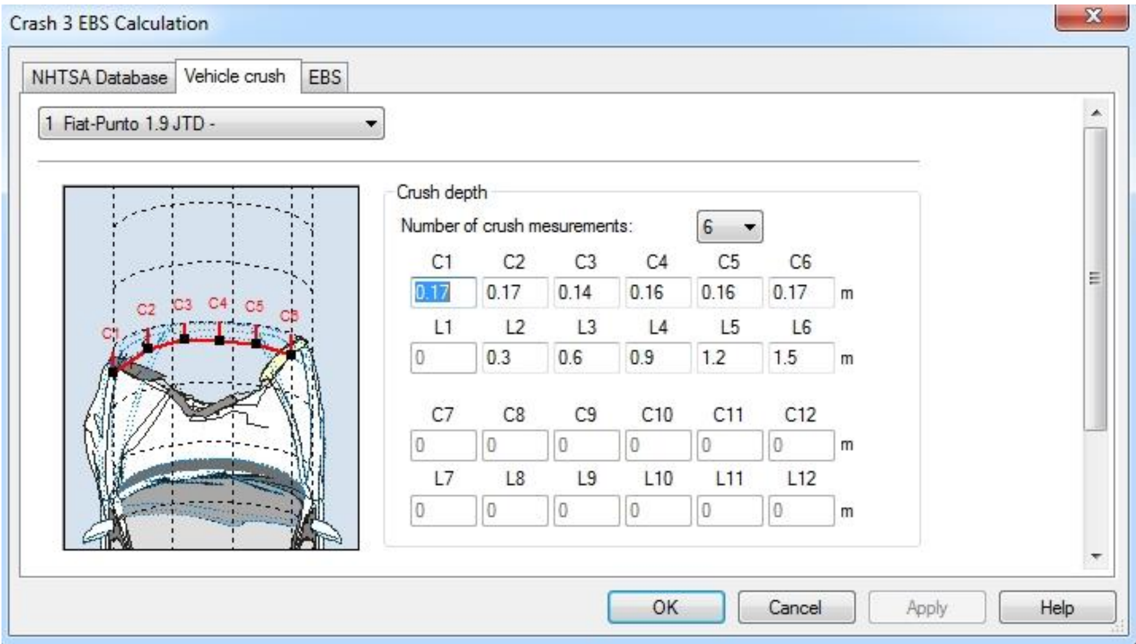

Figure 15. Defining the damage

After the damages of the front part of the vehicle are defined, in the last tab, and based on the data collected from the crash test, energy lost on deformation in a process of collision Ed is calculated, and based on that, EBS values are calculated as well. If necessary, correct the EBS value by entering Θangle of impact force deviation of the vehicle longitudinal axis.

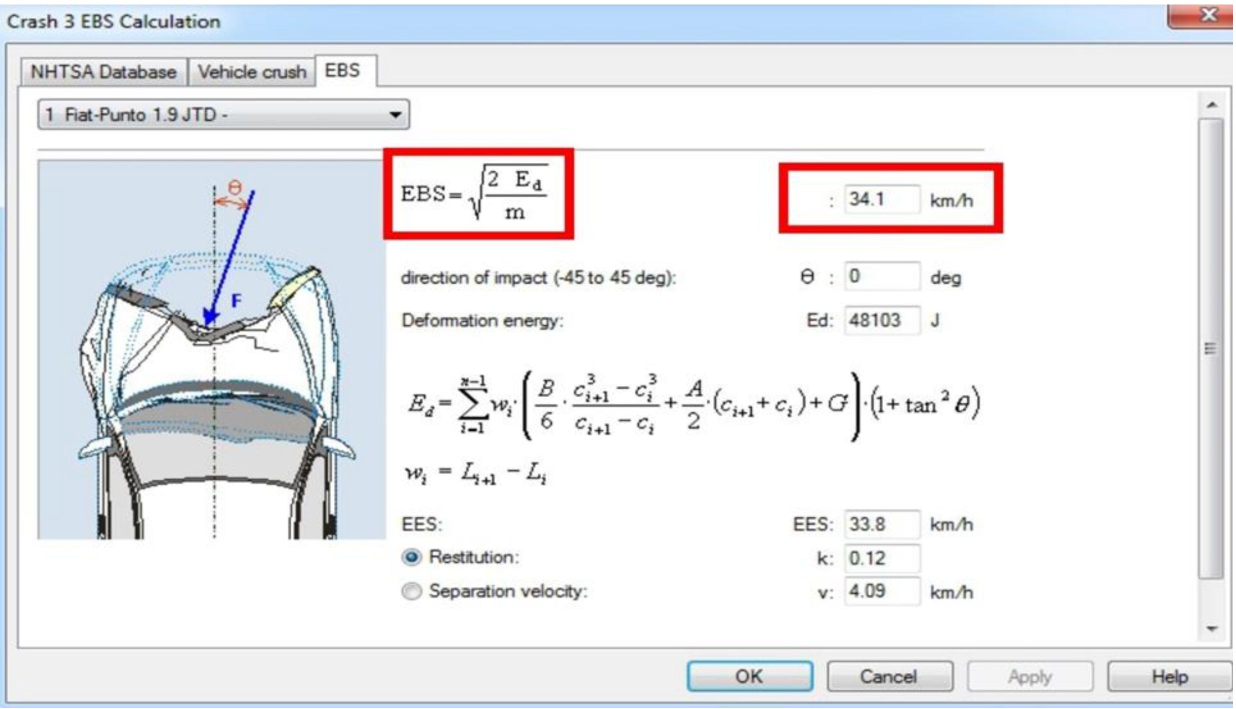

Figure 16. Calculation of deformation energy and EBS values

In our case, the EBS value for damaged vehicle Fiat Punto is 34.1 km/h, while the EES is slightly smaller and is 33.8 km/h.

It was explained that EBS and EES parameters are equivalents of energy dissipated on vehicle deformation (neglecting the work required to e.g. cover the post-crash distance with braking or skidding). But: EES is the velocity at which an impact against a rigid, non-yielding barrier should be performed to get only identical plastic deformation, while EBS additionally takes into account elastic deformation (so EBS≥EES). It is the elastic part that was included in G factor in deformation energy equation Ed.

At the bottom of the box three fields were added:

- EES
- k - coefficient of restitution
- V – vehicle separation velocity difference.

This makes it possible to check what EES value would be if for the velocity of impact against a rigid non-yielding barrier V=EBS coefficient of restitution was k, or alternatively, the difference of vehicles separation velocity was V. The results of EBS or EES calculations are not transferred to any other place in the program.

7. CONCLUSIONS

Photogrammetric method represents one of the fastest methods of data collecting about vehicle geometrics. On the other hand, PhotoModeler package program provides an efficient solution and high quality realistic end results. It is easy to use, but also capable of modeling very complex details with satisfactory preciseness. If to this is added a possibility of creating a 3D model based on photographs from site accident investigation documentation that are made by an unknown camera, then it is clear what advantages has a modern 3D photogrammetry software solution. Apart from a possibility to directly measure damage depth on vehicles, given models can be exported into various formats and further used in CAD programs. Information about damage depth can also be further used for calculations of EES values, position of impact direction, determining mutual damage compatibility, etc. and in combination with software that deal with traffic accident simulations make very powerful tool at court proceedings.

REFERENCES

[1] PhotoModeler Scanner, User manual.

[2] Coyle, F., Digital close-range photogrammetry in motor vehicle accident reconstruction ,Dublin Institute of Technology, 2008.

[3] Burtch, R. Lecture notes-Analytical photogrammetry, The Center for PhotogrammetricTraining, August 2000.

[4] Tomasch E., Accident Reconstruction Guidelines, Graz University of Technology, AT, October 2004.

[5] Wojciech, W., „Simulation of Vehicle Accidents using PC-Crash“, Institute of Forensic Research Publishers, Krakow, 2011, ISBN 83-87425-68-0.

[6] Burg H., Moser A., „Handbuch Verkehrsunfallrekonstruktion“, Friedr. Vieweg & Sohn Verlag | GWV Fachverlage GmbH, Wiesbaden, 2007, ISBN 978-3-8348-0172-2.

MOBILITY & VEHICLE MECHANICS

DOI: 10.24874/mvm.2018.44.01.04
UDC: 629.228:623.87

ELECTRIC KARTING – FROM AN IDEA TO THE REALISATION

Boran Pikula [1*], *Dževad Bibić* [2], *Ivan Filipović* [3], *Mirza Smailbegović* [4]

Received: October 2016 Revised November 2016 Accepted December 2016

RESEARCH ARTICLE

ABSTRACT: It is certain that the first steps of the vehicle drives each individual person were made in karting vehicle. Additional adrenaline and increase driving pleasure gives extremely high noise and the smell of combustion products that may still endure when the ride takes place on an open track during sunny days. However, for many years karting rides take place indoors where it is necessary to provide a special ventilation system for undesirable combustion products. In order to avoid problems of air pollution indoors, reduce noise, and raise awareness of young generations in terms of preservation of the environment, today is increasingly use of electric karting. Having in mind the multiple benefits of electric drive, a reconstruction of karting vehicle with petrol engine into electric karting is presented in the paper. A special attention was paid to the selection of the electric powertrain and battery storage units for electricity, as well as dynamic characteristics of the reconstructed electric vehicle.

KEY WORDS: electric karting, ecology

ELEKTRIČNI KARTING – OD IDEJE DO REALIZACIJE

REZIME: Sigurno je da su prvi koraci vožnje vozila svake osobe zasebno napravljene u karting vozilu. Dodatni andrenalin i povećanje zadovoljstva u vožnji daje izuzetno veliku buku i mirise procesa sagorevanja koji ostaju kada se vožnja odvija na otvorenoj stazi tokom sunčevih dana. Međutim, već dugi niz godina karting vožnja se odvija u zatvorenom prostoru gde je neophodno obezbediti poseban ventilacioni sistem za nepoželjne produkte sagorevanja. Da bi se izbegli problemi zagađenja vazduha u zatvorenom, smanjila buka i podigla svest mladih generacija u smislu očuvanja životne sredine, danas se sve više koristi električni karting. Imajuci u vidu višestruke prednosti električnog pogona, u radu je prikazana rekonstrukcija karting vozila sa benzijskim motorom u električni karting. Posebna pažnja je posvećena odabiru električnog pogona i akumulatorske jedinice za električnu energiju, kao i dinamičkoj karakteristici rekonstruisanog električnog vozila.

KLJUČNE REČI: elektirčni karting, ekologija

[1] *Boran Pikula, Ph.D., Assoc. prof., University of Sarajevo, Faculty of Mechanical Engineering, Department of Motor Vehicles, Vilsonovo šetalište 9, 71000 Sarajevo, Bosna i Hercegovina, pikula@mef.unsa.ba (*Corresponding author)*
[2] *Dževad Bibić, Ph.D., Assoc. prof., University of Sarajevo, Faculty of Mechanical Engineering, Department of Motor Vehicles, Vilsonovo šetalište 9, 71000 Sarajevo, Bosna i Hercegovina, bibic@mef.unsa.ba*
[3] *Ivan Filipović, Ph.D. prof.., University of Sarajevo, Faculty of Mechanical Engineering, Department of Motor Vehicles, Vilsonovo šetalište 9, 71000 Sarajevo, Bosna i Hercegovina, filipovic@mef.unsa.ba*
[4] *Mirza Smailbegovic, University of Sarajevo, Faculty of Mechanical Engineering, Department of Motor Vehicles, Vilsonovo šetalište 9, 71000 Sarajevo, Bosna i Hercegovina*

Intentionally blank

ELECTRIC KARTING – FROM AN IDEA TO THE REALISATION

Boran Pikula, Dževad Bibić, Ivan Filipović, Mirza Smailbegović

1. INTRODUCTION

The first steps that every young person made in the drive of a motor vehicle are related with karting which is usually powered by the petrol engine. In order to achieve relatively good dynamic characteristics in forms of acceleration and top speed, the greatest problem when using these vehicles is the large emissions of pollutants and the noise. Furthermore, this problem is partly solved in case when the karting is used on open tracks where excellent weather conditions with no rain are generally required. However, in our region it implies usually semi-annual period, from mid-April to mid-October.

In order to enable the younger generations the use karting throughout the year, recently enclosed areas are used, specially prepared for driving karting vehicle, where special attention is paid to the ventilation space, the increased noise and high-quality surface. Finally, more attention is drawn to electric karting vehicle, which definitely has no problem with emissions of pollutants and noise. Today one can meet karting electric vehicles that are specially making for this purpose, but the question is whether the same vehicle to be reached by reconstructing existing karts with petrol engine. The answer to this question is given in this paper.

2. REDESIGN OF EXISTING PETROL KARTING

As the basis for the redesign, a classic karting with a petrol engine with 5 kW powered is used, which is shown in the Figure 1.

Figure 1. A classic existing karting with petrol engine

In order to make modification in to electric karting, from a classic karting, the gas tank and the gasoline engine were removed, and instead of these components there is a need for deployment electrical components. With the objective of maintaining a similar dynamic performance, the BLDC synchronous electric motor by company Golden Motor [1] was elected, with the power of 5 kW, voltage 48 V and its controller 48 V / 360 A, accelerator pedal and the other components. Drive of electric motor is achieved by Li-Fe-Po battery with 16 cells, a single voltage of 3.2 V, which ultimately provides a total voltage in the range of 44.8 to 51.2 V. In order to symmetry loads, the batteries are arranged on the left and right side of the driver in special carriers, and connected in series to provide a nominal voltage of 48 V. The redesigned karting is given in the Figure 2.

Figure 2. The electric karting and scheme of electrical installation

As has been mentioned, the greatest problem in designing electric karting was location of batteries and getting symmetrical loads on the left and right side. Finally, the 16-cell battery, divided into 8 to the left and 8 to the right, and their fixation is ensured by the use of specific carriers. These carriers have been implemented in the form of boxes and placed on the left and right side of the driver's seat, which can be seen in the Figure 3. In order to increase security, in terms of avoiding a side impact in the Li-Fe-Po battery and possible leakage and explosion, side protectors are retained additional.

An additional challenge for the redesigned construction of electric karting chassis has been making an electric motor carrier. Having in mind that there are no present torsional oscillations about the axis on the electric motor, a support structure is performed by a plate that is specifically placed and welded to the rest of the chassis structure, which is also seen in the Figure 3. The entire structure of karting chassis is loaded realistic with the associated loads (driver, battery, electric motor, electrical installation, etc.), while using a computer program Solid works [2], the appropriate strains and deformations have been obtained. The Figure 4 shows the loads of the structure in terms of the factor of safety.

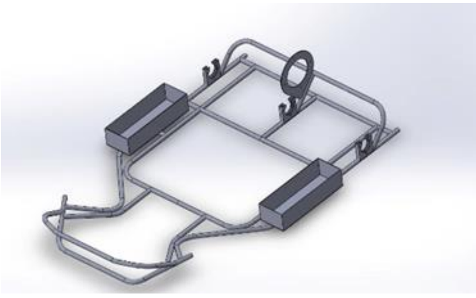

Figure 3. Redesigned model of karting chassis

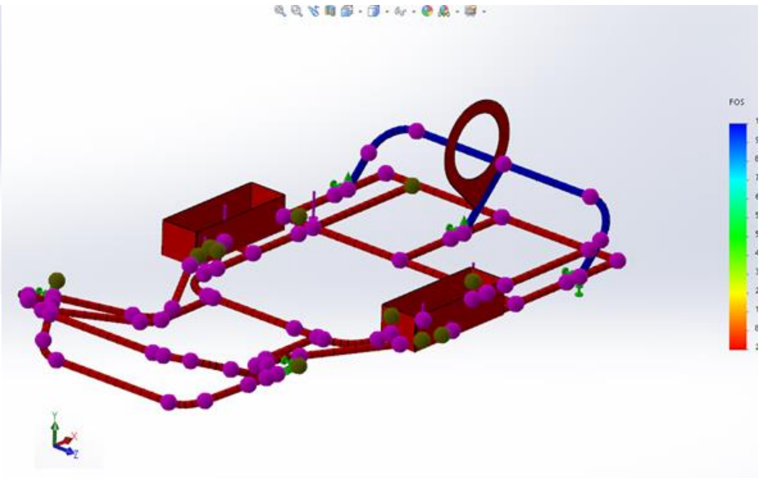

Figure 4. Structural analysis of karting chassis – factor of safety

3. INVESTIGATION OF DYNAMIC CHARACTERISTICS

After completion of the numerical and mathematical calculations, it is started with the specific modifications on karting, setting the battery, electromotor and other electrical installations. The final design of electric karting is shown in the Figure 2. A special attention was dedicated to the study of dynamic characteristics of electric karting [3]. The investigations of the dynamic characteristics was performed on the test track near the Airport Mostar [4]. In these experiments, an acceleration time during 10 consecutive measurements, then achieving maximum speed and check the stability of the karting during motion in the slalom test were defined. The results of 10 consecutive acceleration to speed of 50 km/h are shown in the Figure 5. To define the dynamic characteristics of electric karting, the GPS device manufactured by company Racelogic [5], model VBOX sport, with frequency of 20 Hz and precision in measurement of speed of 0.1 km/h was used.

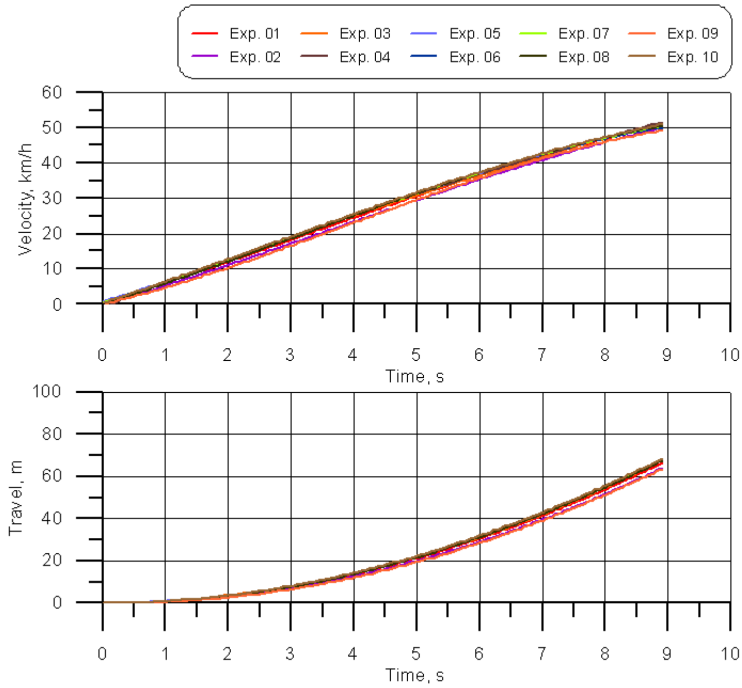

Figure 5. Velocity and travel of electric karting during acceleration tests

Based on these results one can conclude that all measurements were made within the required limits. It leads to the conclusion that used batteries can provide a safe and quality supply to electric motor during successive tests and almost the same results during accelerations.

Figure 6. Acceleration test on the test track

Figure 7. Slalom test on the test track

During testing on the test track it was found that the maximum speed of the electric karting is almost 90 km/h. In order to achieve the maximum speed the necessary time is almost 35 s. Successful mastering of the slalom test was carried out at a speed of 72 km/h, which is due to low center of gravity and a relatively large distance between the cones of 18 m.

4. CONCLUSIONS

This project demonstrate a successful procedure of making the first electric karting in Bosnia and Herzegovina. In realization of this project, the basis was existing karting with petrol engine. The second step was selection and buying electrical equipment (electromotor, batteries and other electrical installation). Finally, the existing karting was redesigned and all electrical equipment was placed on the karting chassis. Price of reconstruction amounted to 4,000 € which is significantly less than the cost of new electric karting which are offered on the market. The dynamic characteristics of electric karting are excellent. The electric karting is the great idea for use in halls (closed spaces) during winter season because there are no toxic air pollution with small noise. A one problem could be the duration of the batteries life per cycle, in the case of long lasting use. From this reason it is suggested to insure another set of batteries for all day use.

ACKNOWLEDGMENTS

The project to create the first electric karting in Bosnia and Herzegovina was conducted during 2014. The realization of this project in addition to the staff of Mechanical Engineering Faculty in Sarajevo attended by the staff of Faculty of Electrical Engineering in Sarajevo, and the following companies: Auto Media Group Ltd., Auto Expert Ltd., Bosnjak EV Ltd. Authors use this opportunity to express thanks to the Ministry of Civil Affairs of Bosnia and Herzegovina for financial support in realisation of this project. (Contract No. 10-35-5-675/13-34 dated December 18, 2013).

REFERENCES

[1] Golden Motors, http://www.goldenmotor.com, accessed on 2014-09-07.

[2] Solid works: “User Manual”, 2012.

[3] Dacić S., Trobradović M., Pikula B: „Osnovi dinamike vozila – zbirka zadataka“, Mašinski fakutet Sarajevo, Sarajevo, 2008.

[4] Gadžo A.: “Procedure ispitivanja dinamičkih karakteristika vozila - diplomski rad“, Mašinski fakultet Sarajevo, Sarajevo, 2012.

[5] Racelogic: “VBox sport – User Manual”, Racelogic, UK, 2011.

MOBILITY & VEHICLE MECHANICS

DOI: 10.24874/mvm.2018.44.01.05
UDC: 629.25

RESEARCH THE INFLUENCE OF SPARK PLUGS TYPES ON THE PERFORMANCE OF THE ENGINE OPERATING ON GASEOUS FUELS

Rosen Hristov [1], Krasimir Bogdanov [2], Radostin Dimitrov [3]*

Received: February 2018 Revised: May 2018 Accepted June 2018

RESEARCH ARTICLE

ABSTRACT: Topical issue in recent years is the search for methods of reducing fuel consumption and improve environmental performance of internal combustion engines. In spark-ignition engines great importance is the type of ignition system and its components. This report examined the performance of the internal combustion engine running on gaseous fuels and with different types of spark plugs. Presented are the power-economic and environmental characteristics of different fuels and different types of spark plugs. Conclusions are practical and economic terms..

KEY WORDS: spark plug, LPG, CNG, ICE, performance

ISTRAŽIVANJE UTICAJA TIPOVA SVEĆICA NA PERFORMANSE RADA MOTORA SA GASNIM GORIVIMA

REZIME: Aktuelno pitanje poslednjih godina je potraga za metodama smanjenja potrosnje goriva i poboljsanja ekoloske performanse motora sa unutrasnjim sagorevanjem. U motorima sa paljenjem svecicama, vazan je tip sistema paljenja i njegove komponente. Ovaj izvestaj je ispitivao performanse motora sa unutrasnjim sagorevanjem probanjem različitih gasnih goriva i sa različitim tipovima svećica. Predstavljene su energijsko-ekonomske i ekološke karakteristike razlicitih goriva i različitih tipova svećica. Zaključci su praktični i ekonomski uslovi.

KLJUČNE REČI: svećica, LPG, CNG, ICE, performanse

[1]*Rosen Hristov, Ph.D., Assoc. prof., Technical University Varna, Bulgaria 9010, Varna, 1Studentska Str., rosen.hristov@tu-varna.bg (*Corresponding author)*
[2]*Krasimir Bogdanov, Ph.D., Assoc. prof., Technical University Varna, Bulgaria 9010, Varna, 1Studentska Str., kbog@abv.bg*
[3]*Radostin Dimitrov, Senior Assist. Lecturer, Technical University Varna, Bulgaria 9010, Varna, 1Studentska Str., r_dimitrov@tu-varna.bg*

Intentionally blank

RESEARCH THE INFLUENCE OF SPARK PLUGS TYPES ON THE PERFORMANCE OF THE ENGINE OPERATING ON GASEOUS FUELS

Rosen Hristov, Krasimir Bogdanov, Radostin Dimitrov

1. INTRODUCTION

Despite the low prices of the oil in the recent years the gaseous fuels continue to be widely used as an alternative to the traditional liquid fuels. In most cases, when transforming engines so as to be able to operate with gaseous fuels, we speak about vehicles with significant mileage. As regards those vehicles, the main objective is to ensure the proper and normal operation of the engine ignition system. The question what type of spark plugs to be used - the standard ones recommended by the manufacturer of the vehicle or spark plugs intended specifically for gaseous fuels - is raised. In the recent years, the iridium spark plugs for which the manufacturers promise better performance of the engines using them and longer life of the spark plugs themselves have become widely popular. This study puts the beginning of the implementation of a more comprehensive project covering spark plugs manufactured by the most leading companies and several types of gaseous fuels.

2. SUBJECT OF RESEARCH

In the operation of internal combustion engines with external carburation and positive ignition it is essential to provide reliable combustion of the gaseous mixture in the cylinder space. This is mainly determined by several factors:

- technical condition of the engine
- composition of the fuel-air mixture
- quality of the electrical spark
- condition of the ignition system
- type of fuel used.

We will not comment on the impact of the engine technical condition, since it is clear that the engine must be in a full working order.

The use of gaseous fuels for operation of internal combustion engines has some features which must be taken into account in the choice of gas modified ignition system:

1. It is known that the flashpoint of the various fuels is different and varies:
    - Methane it is 545 - 800°C
    - Ethane - 530 - 694°C
    - Propane - 504 - 588°C
    - Propylene - 455 - 550°C
    - N-butane - 430 - 570°C
    - Isobutane - 490 - 510°C
    - Isobutylene - 400 - 440°C
    - Gasoline - 480 - 530°C.

This means that a high energy ignition system (especially when working with methane) must be used for the gaseous fuel ignition.

2. To obtain effective and cost-efficient operation of the engine using gaseous fuel leaner mixtures must be used. This requires that high effective and reliable ignition system should be used to ensure the timely combustion of the aggregated fuel-air mixture.

A spark plug (figure1) is composed of a shell, insulator and the central conductor. It passes through the wall of the combustion chamber and therefore must also seal the combustion chamber against high pressures and temperatures without deteriorating over long periods of time and extended use.

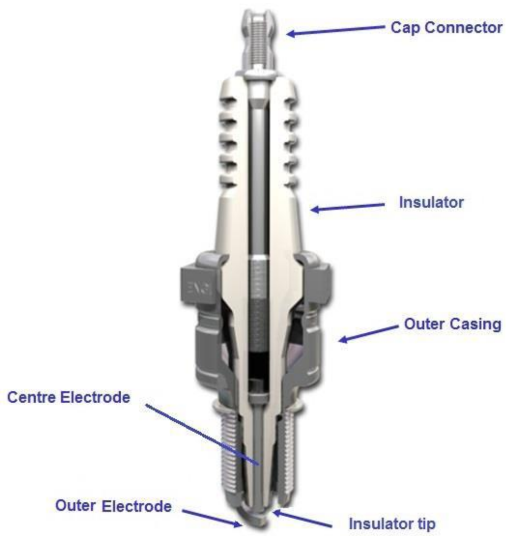

Figure 1. Spark plug construction

A modern spark plug must meet the following requirements:

- Reliable high-voltage transmission, even at ignition voltages of up to 40,000 volts;
- Good insulation capability, even at temperatures of 1,000 °C, prevention of arcing and flashover;
- Resistance to thermal shock (hot exhaust gases – cold intake mixture);
- Good thermal conduction by insulator tip and electrodes;
- Pressure-tight and gas-tight sealing of the combustion chamber, resistance to oscillating pressures up to approx. 100 bar;
- High mechanical strength for reliable installation;
- Resistance to spark erosion, combustion gases and residues;
- Prevention of build-up of deposits on the insulator.

The thermal rating is a measure of the thermal structure of a spark plug. It indicates the maximum thermal loading on the spark plug in equilibrium between heat absorption and heat dissipation. It is vital to choose the correct thermal rating when selecting a spark plug. The central electrode is connected to the terminal through an internal wire and commonly a ceramic series resistance to reduce emission of RF noise from the sparking. Non-resistor spark plugs, commonly sold without an "R" in the plug type part number, lack this element to reduce electro-magnetic interference with radios and other sensitive equipment. The tip can be made of a combination of copper, nickel-iron, chromium, or noble metals.

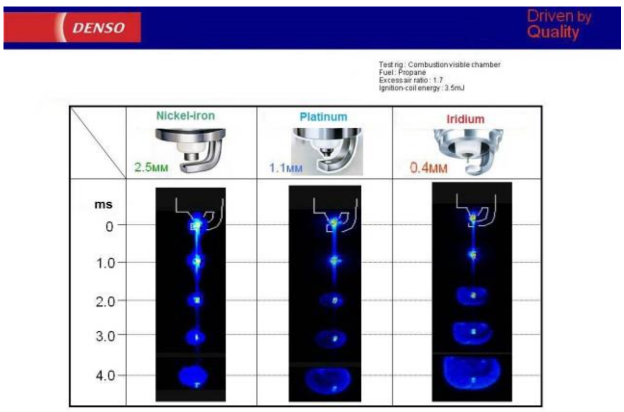

Figure 2. Flame speed at different Spark plugs

The development of noble metal high temperature electrodes (using metals such as yttrium, iridium, tungsten, or palladium, as well as the relatively high value platinum, silver or gold) allows the use of a smaller center wire, which has sharper edges but will not melt or corrode away. These materials are used because of their high melting points and durability, not because of their electrical conductivity (which is irrelevant in series with the plug resistor or wires). The smaller electrode also absorbs less heat from the spark and initial flame energy (figure 2). Some of the characteristics of metals are shown in Table 1.

Table 1. Metal characteristics

Material	Melting point [°C]	Hardness [Hv]	Strength [kg/mm^2]
Iridium	2450	450	110
Platinum	1770	50	15
Nickel	1450	160	70

3. RESULTS AND DISCUSSION

The map dependent value determined based on the composition of the fuel-air mixture at 3,400 rpm and partial throttle has been presented. Liquefied petroleum gas (LPG) and compressed natural gas (CNG) are used as fuels to operate the engine Rover 1.3. We use different spark plugs (figure 3) - regular nickel Denso, iridium Denso, especially designed for gas fuels silver Brisk and platinum iridium Bosch. These spark plugs cover different price range and reputation.

Figure 3. Spark plugs used in our experimental research

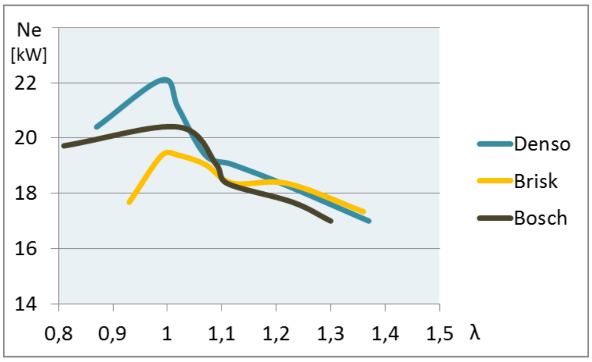

Figure 4. Effective power, fuel CNG

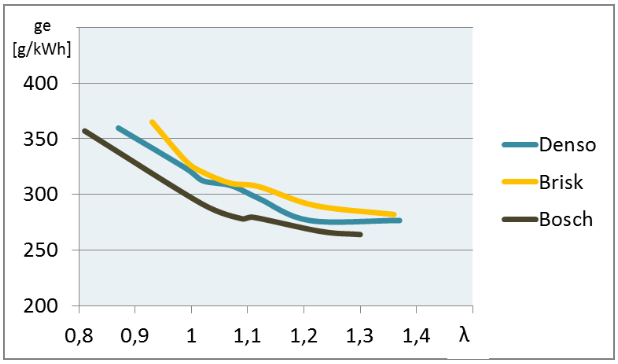

Figure 5. Effective specific fuel consumption, fuel CNG

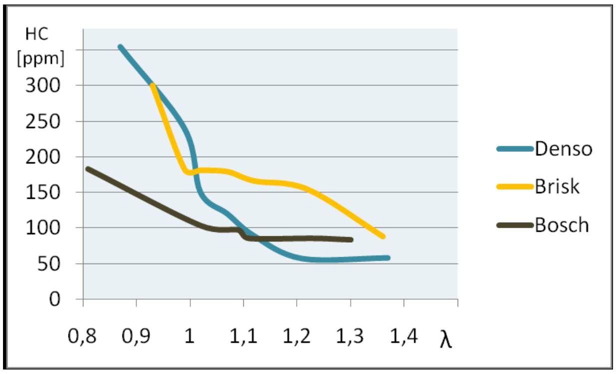

Figure 6. Hydrocarbon emissions, fuel CNG

The change of the engine effective power based on the change of the map dependent value – figure 4 - shows that if the fuel-air mixture has a stoichiometric composition and if spark plugs Denso are used the maximum power is 22.1 kW; if spark plugs Bosch are used the maximum power is 20.4 kW, and if spark plugs Brisk are used the maximum power is 19.3 kW. The effective specific fuel consumption (ge) – figure 5 - is significantly affected by the type of spark plug at low air–fuel equivalence ratio which means: lowest value is for spark plugs Bosch, consumption for spark plug Denso and Brisk is respectively 6.2% and 14 % more.

Figure 6 shows the change of the hydrocarbon amount (HC) in the exhaust gases. Higher values are reported when CNG is used (140 ÷ 235 ppm), while the values reported when the engine is operated by LPG are 65 ÷ 125 ppm.

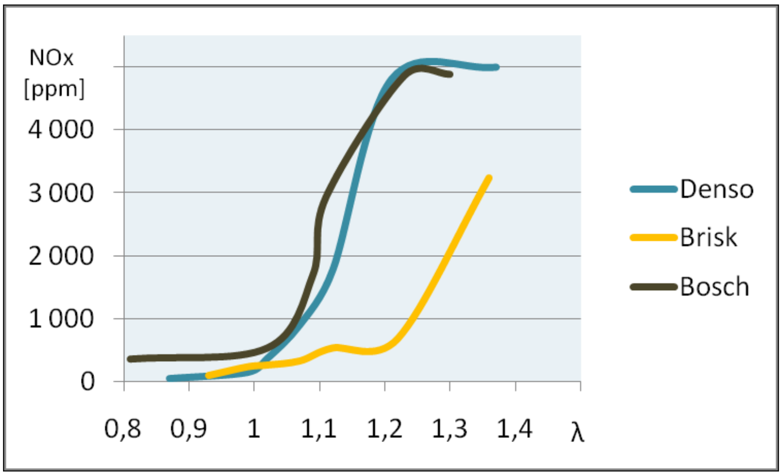

Figure 7. Mono-nitrogen oxides emissions, fuel CNG

The nitrogen oxides grow with the increase in fuel air ratio, as lowest are at spark plugs Brisk (figure 7). The values are changing from 89 to 3233 ppm for Brisk, from 42 to 4999 ppm for Denso and from 351 to 4880 ppm for Bosch.

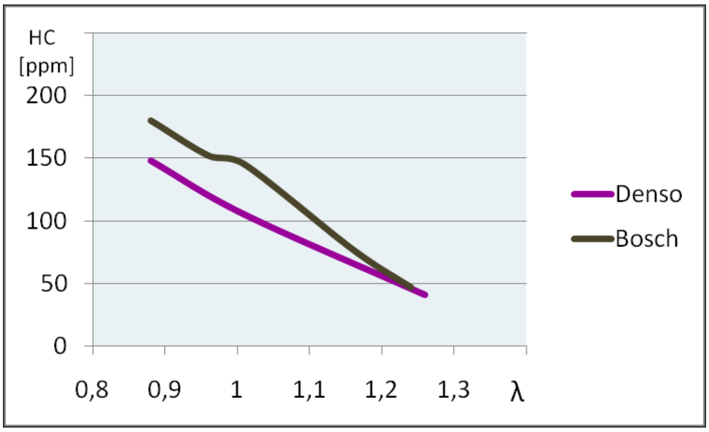

Figure 8. Hydrocarbon emissions, fuel LPG

Experiments were performed on a comparison of the two types of iridium spark plugs (Bosch and Denso) by fuel LPG. There hasn't significant difference in the power and economic engine performance. Visible differences has only in the toxicity of exhaust emissions especially in hydrocarbons (figure 8). The values are changing from 41 to 148 ppm for Denso and from 47 to 180 ppm for Bosch.

4. CONCLUSIONS

- With fuel CNG higher engine power close to the stoichiometric fuel-air mixture is achieved when the engine is equipped with spark plugs Denso. Lowest hourly fuel consumption is achieved when spark plugs Bosch are used.
- As regards the environmental performance, lowest hydrocarbon emissions are reported when spark plugs Bosch are used, as only in case of large amount of lean fuel-air mixture the use of spark plugs manufactured by Denso leads to lower hydrocarbon emissions. Lowest nitrogen oxide emissions are reported when spark plugs Brisk are used.
- When natural gas is used the type of spark plugs have greater importance for the performance and emissions of the engine compared to LPG
- Comprehensive and more detailed studies must be conducted to conclusively determine the advantages of the spark plugs intended specifically for engines operated with gaseous fuels.

ACKNOWLEDGMENTS

The research results of which are presented in this publication are made on the project within the inherent TU - Varna research funded by the state budget target.

REFERENCES

[1] Ahmed A., Impact of spark plug number of ground electrodes on engine stability, Ain Shams Engineering Journal, 2013, 4(2), 307-316, doi: 10.1016/j.asej.2012.09.006.

[2] Hristov R., Influence of the type of spark plugs on the combustion process, Proceedings of the International Conference Trans&Motauto '09, 2009, 98-100.

[3] Meyer R., Meyers D., Effects of Spark Plug Number and Location in Natural Gas Engines, J. Eng. Gas Turbines Power, 1992, 114(3), 475-479.

[4] Osamura H. et al., Development of New Iridium Alloy for Spark Plug Electrodes, SAE paper 1999-01-0796, 1999.

[5] Timtamand P., Parnklang J.,Multi Time Ignition Concept of Four Stoke Gasoline Engine, Proceedings of the International Multi Conference of Engineers and Computer Scientists, Hong Kong, IMECS, 2016, 1,486, ISBN: 978-988-19253-8-1.

[6] Yorita, H., Okabe, H., Hiroya, I., Shibata, M., Ignition simulation and visualization for spark plug electrode design, SAE paper 2007-01-0940, 2007, doi: https://doi.org/10.4271/2007-01-0940.

NOTIFICATION TO AUTHORS

The Journal MVM publishes original papers which have not been previously published in other journals. This is responsibility of the author. The authors agree that the copyright for their article is transferred to the publisher when the article is accepted for publication.

The language of the Journal is English.

Journal ***Mobility & Vehicles Mechanics*** is at the SSCI list.

All submitted manuscripts will be reviewed. Entire correspondence will be performed with the first-named author.

Authors will be notified of acceptance of their manuscripts, if their manuscripts are adopted.

INSTRUCTIONS TO AUTHORS AS REGARDS THE TECHNICAL ARRANGEMENTS OF MANUSCRIPTS:

Abstract is a separate Word document, "*First author family name_ABSTRACT.doc*". Native authors should write the abstract in both languages (Serbian and English). The abstracts of foreign authors will be translated in Serbian.

This document should include the following: 1) author's name, affiliation and title, the first named author's address and e-mail – for correspondence, 2) working title of the paper, 3) abstract containing no more then 100 words, 4) abstract containing no more than 5 key words.

The manuscript is the separate file, „*First author family name_Paper.doc*" which includes appendices and figures involved within the text. At the end of the paper, a reference list and eventual acknowledgements should be given. References to published literature should be quoted in the text brackets and grouped together at the end of the paper in numerical order.

Paper size: Max 16 pages of B5 format, excluding abstract
Text processor: Microsoft Word
Margins: left/right: mirror margin, inside: 2.5 cm, outside: 2 cm, top: 2.5 cm, bottom: 2 cm
Font: Times New Roman, 10 pt
Paper title: Uppercase, bold, 11 pt
Chapter title: Uppercase, bold, 10 pt
Subchapter title: Lowercase, bold, 10 pt
Table and chart width: max 125 mm
Figure and table title: Figure _ (Table _): Times New Roman, italic 10 pt

Manuscript submission: application should be sent to the following e-mail:

mvm@kg.ac.rs ; lukicj@kg.ac.rs
or posted to address of the Journal:
University of Kragujevac – Faculty of Engineering
International Journal M V M
Sestre Janjić 6, 34000 Kragujevac, Serbia

The Journal editorial board will send to the first-named author a copy of the Journal offprint.

OBAVEŠTENJE AUTORIMA

Časopis MVM objavljuje orginalne radove koji nisu prethodno objavljivani u drugim časopisima, što je odgovornost autora. Za rad koji je prihvaćen za štampu, prava umnožavanja pripadaju izdavaču.

Časopis se izdaje na engleskom jeziku.

Časopis ***Mobility & Vehicles Mechanics*** se nalazi na SSCI listi.

Svi prispeli radovi se recenziraju. Sva komunikacija se obavlja sa prvim autorom.

UPUTSTVO AUTORIMA ZA TEHNIČKU PRIPREMU RADOVA

Rezime je poseban Word dokument, "*First author family name_ABSTRACT.doc*". Za domaće autore je dvojezičan (srpski i engleski). Inostranim autorima rezime se prevodi na srpski jezik. Ovaj dokument treba da sadrži: 1) ime autora, zanimanje i zvanje, adresu prvog autora preko koje se obavlja sva potrebna korespondencija; 2) naslov rada; 3) kratak sažetak, do 100 reči, 4) do 5 ključnih reči.

Rad je poseban fajl, „*First author family name_Paper.doc*" koji sadrži priloge i slike uključene u tekst. Na kraju rada nalazi se spisak literature i eventualno zahvalnost. Numeraciju korišćenih referenci treba navesti u srednjim zagradama i grupisati ih na kraju rada po rastućem redosledu.

Dužina rada: Najviše 16 stranica B5 formata, ne uključujući rezime
Tekst procesor: Microsoft Word
Margine: levo/desno: mirror margine; unurašnja: 2.5 cm; spoljna: 2 cm, gore: 2.5 cm, dole: 2 cm
Font: Times New Roman, 10 pt
Naslov rada: Velika slova, bold, 11 pt
Naslov poglavlja: Velika slova, bold, 10 pt
Naslov potpoglavlja: Mala slova, bold, 10 pt
Širina tabela,dijagrama: max 125 mm
Nazivi slika, tabela: Figure __ (Table _): Times New Roman, italic 10 pt

Dostavljanje rada elektronski na E-mail: **mvm@kg.ac.rs ; lukicj@kg.ac.rs**

ili poštom na adresu Časopisa
Redakcija časopisa M V M
Fakultet inženjerskih nauka
Sestre Janjić 6, 34000 Kragujevac, Srbija

Po objavljivanju rada, Redakcija časopisa šalje prvom autoru jedan primerak časopisa.

MVM *Editorial Board*
University of Kragujevac
Faculty of Engineering
Sestre Janjić 6, 34000 Kragujevac, Serbia
Tel.: +381/34/335990; Fax: + 381/34/333192
www.mvm.fink.rs